

### 3.6.2. Inverse Methods

JAN W. HOPMANS, *University of California, Davis, California*

JIRI ŠIMŮNEK, *George E. Brown Jr. Salinity Laboratory, Riverside, California*

NUNZIO ROMANO, *University of Naples “Federico II”, Naples, Italy*

WOLFGANG DURNER, *Braunschweig Technical University, Braunschweig, Germany*

#### 3.6.2.1 Introduction

An adequate hydrological description of water flow and contaminant transport in the vadose zone relies heavily on soil water retention and unsaturated hydraulic conductivity data of the considered spatial domain. The importance of an accurate soil hydraulic description of the vadose zone, including the root zone, is increasingly recognized in the fields of environmental engineering, soil physics and groundwater hydrology. With the current focus on the entire vadose zone, with increasing applications of watershed and land-atmosphere models, the spatial and temporal scales of interest have shifted to larger dimensions. This trend in increasing larger spatial scales brings along with it the presence of increasing soil heterogeneity. Hence, methodologies need to be available that allow for a rapid and accurate soil hydraulic characterization, including its spatial variability.

Currently, many laboratory and field methods exist to determine the highly nonlinear soil hydraulic functions in the vadose zone, represented by soil water retention and unsaturated hydraulic conductivity curves. Most methods require either static or steady-state flow conditions to satisfy the assumptions of the corresponding analytical solution, which can make measurements time consuming. Excellent reviews of these types of direct methods are presented by Dirksen (1991), Reeve and Carter (1991), and in Sections 3.3, 3.4, and 3.5 of this book. In contrast, the inverse modeling approach presented here estimates soil hydraulic properties from transient experiments, giving much more flexibility in experimental boundary conditions than required for steady-state methods. As an additional advantage, inverse modeling allows the simultaneous estimation of both the soil water retention and unsaturated hydraulic conductivity function from a single transient experiment. In other ways, inverse modeling of transient water flow is not much different than methods applied to steady flow. In either case, inversion of the governing equation is required to estimate the unsaturated hydraulic conductivity function from experimental data. Whereas the steady-state methods invert Darcy's equation, transient methods invert Richards' equation. Inversion of Richards' equation requires repeated numerical simulation of the governing transient flow problem. Successful application of the inverse modeling technique improves both speed and accuracy, as there is no specific need to attain steady-state flow.

By definition, inverse modeling is a general mathematical method to determine unknown causes on the basis of observation of their effects, as opposed to modeling of direct problems whose solution involves finding effects on the basis of a description of their causes. Inverse modeling is widely accepted in engineering and physical sciences for system characterization. For example, in Section 6.6, inverse modeling is applied to estimate solute transport parameters. In this section, we focus on the application of inverse modeling towards parameter estimation of soil hydraulic functions. Inverse modeling was first applied to the pressure plate outflow method, where an initially saturated soil core was subjected to a series of step increases in air pressure with the drainage or outflow measured after each pressure step increase (Gardner, 1956). Assuming a constant soil water diffusivity within pressure steps, the analytical solution yielded the soil water diffusivity as a function of soil water content. Doering (1965), using Gardner's (1962) solution, simplified the outflow method by proposing a one-step experiment, so that considerable timesaving was achieved without loss in accuracy. Additional modifications were introduced by Passioura (1976), Gupta et al. (1974), and Valiantzas and Kerkides (1990). This last paper extended the outflow method to the simultaneous determination of the soil water retention and unsaturated hydraulic conductivity functions using the Brooks and Corey (1966) formulation of the soil hydraulic properties. Among the first to suggest the application of inverse modeling to estimate soil hydraulic parameters were Whisler and Watson (1968), who suggested the use of drainage volume and the soil water retention curve to estimate the unsaturated conductivity curve of a draining soil by matching observed and simulated drainage flows. Significant progress has been made regarding the nonuniqueness of the optimized parameters and the type of flow variable(s) to be included in the objective function. Zachman et al. (1981) used simulated drainage data to show that the best parameter optimization results were obtained if cumulative drainage flow was matched with predicted outflow. Moreover, in a subsequent paper, Zachman et al. (1982) showed the importance of selecting the correct parametric form for the soil hydraulic functions. Kool and Parker (1988) and Russo et al. (1991) applied this approach to one-dimensional unsaturated flow problems. Their goal was to estimate parameter values for unsaturated porous media in laboratory soil columns. Kool and Parker (1988) discussed the advantage of including tensiometric data in the inverse approach, measured simultaneously with drainage rates for a hypothetical infiltration and redistribution experiment.

The inverse modeling approach assumes a priori that the applied process model and the selected hydraulic relationships are an exact description of the soil's physical behavior, and therefore assumes that the model error is negligible. This implies that deviations between simulation and observation are caused only by randomly distributed inaccuracies of measurements. Russo (1988) studied the influence of the parametric form of the soil hydraulic functions on the one-step outflow optimization. For that purpose he investigated the Mualem–van Genuchten (van Genuchten, 1980), Brooks and Corey (1966), and Gardner–Russo (Russo, 1988) soil hydraulic models, using data from Kool et al. (1985) and Parker et al. (1985). In a subsequent paper, Russo et al. (1991) pointed out that the larger number of parameters in the van Genuchten model might enhance the likelihood of nonuniqueness and instability in the inverse solution. Also, Chen et al. (1999) tested seven differ-

ent soil hydraulic models in their ability to fit multistep outflow experimental data, and concluded that only four of these models were able to describe the outflow data successfully.

Although laboratory experiments have the advantage of being quick and precise, they often lead to soil hydraulic properties that are not representative of the field. Among the benefits of inverse methods is the fact that they are equally applicable to field experiments, even under nontrivial boundary conditions. The first application of the inverse problem to field data was conducted by Dane and Hruska (1983), in which the parameters of van Genuchten's (1980) soil hydraulic functions were optimized from transient drainage data. An in-depth discussion of the application of the inverse parameter estimation method as applied to field experiments is presented by Kool et al. (1987) and Kool and Parker (1988).

The objective of this section is to introduce the reader to the theory and applications of inverse modeling for parameter estimation of soil hydraulic functions, using various proven experimental techniques. New developments are continuously made, so this discussion must be regarded as "work in progress". In any case, inverse modeling in general has been shown to be an exciting new tool that allows for soil hydraulic characterization using a wide spectrum of transient laboratory and field experiments.

In the subsequent sections we summarize the recent developments in various laboratory and field techniques to indirectly determine soil hydraulic properties using the inverse method. First, we introduce the reader to the basic theoretical concepts underlying all presented applications of inverse modeling for hydraulic parameter estimation. For a better understanding of this theoretical background, we recommend to first read the general review of the application and theory of parameter optimization in Section 1.7. Subsequently, we discuss specific established experimental methods for hydraulic parameter estimation. The experiments by themselves are reviewed elsewhere (e.g., Sections 3.3, 3.5, and 3.6.1); however, the type and number of measurements may need to be adapted to better serve the inverse methodology. Accordingly, issues that relate to the analysis and interpretation of the parameter estimation results (both simulation and optimization modeling) will be specifically addressed. Finally, we will introduce a step-by-step example of the inverse method, analyzing the influence of experimental conditions on parameter optimization results.

### 3.6.2.2 Theory of Flow and Optimization

The inverse method includes three interrelated functional parts (Fig. 3.6.2-1): (i) a controlled transient flow experiment for which boundary and initial conditions are prescribed and various flow variables are measured, such as cumulative infiltration and/or drainage cumulative and/or matric head and/or water content; (ii) a numerical flow model simulating the transient flow regime of this experiment, using initial estimates of the parametric soil hydraulic functions; and (iii) an optimization algorithm, which estimates the unknown parameters through minimization of the difference between observed and simulated flow variables (residuals) defined in an objective function ( $\Phi$ ) through an iterative solution of the transient flow equation. The quality of the final solution of the parameter estimation problem is de-

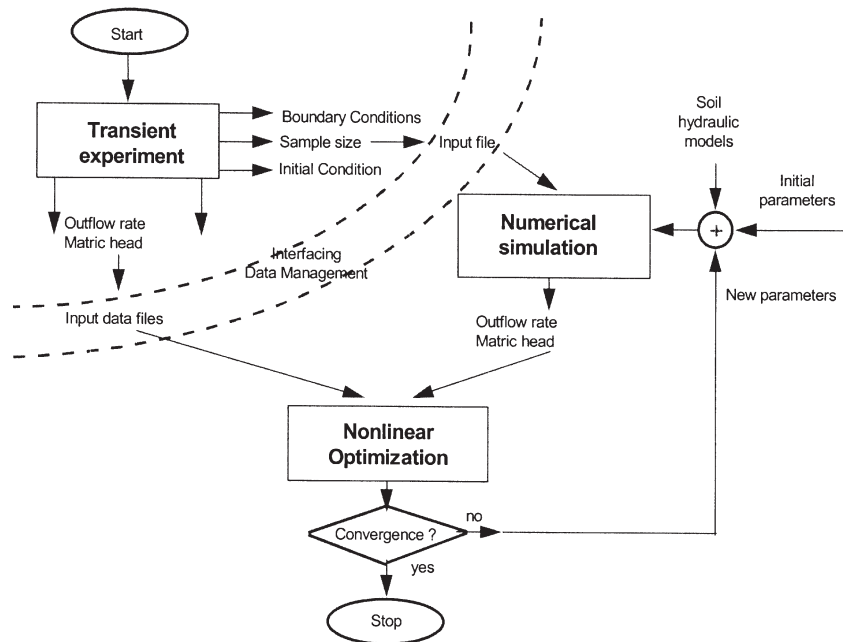


Fig. 3.6.2-1. Flow chart of the inverse method illustrating the integration of measurement, modeling, and optimization (modified from Hopmans & Simunek, 1999).

pendent on each of these three individual components as well as their integration within a computational framework. The three components are interfaced through data files that include experimental, numerical flow model, and parameter optimization results. Parameters of the soil hydraulic functions are updated iteratively in the optimization routine, thereby continuously reducing the residuals until a pre-determined convergence criterion (e.g., reduction in  $\phi$  value between two consecutive iterations) has been achieved. As any other soil hydraulic characterization method, the magnitude of the residuals in the objective function will depend on the proper selection of the soil hydraulic model; that is, an inappropriate model will increase deviations between measurements and simulations. In this section we describe the water flow simulation and parameter optimization components, and elaborate on the consequences of implied assumptions.

### 3.6.2.2.a Water Flow Modeling

One-dimensional vertical variably saturated water flow in soils is usually described using Richards' equation:

$$\partial\theta/\partial t = (\partial/\partial z)[K(h_m)(\partial h_m/\partial z) + K(h_m)] \quad [3.6.2-1]$$

where  $\theta$  denotes the volumetric water content ( $L^3 L^{-3}$ ),  $h_m$  is the soil water matric head (L),  $K$  is the unsaturated hydraulic conductivity ( $L T^{-1}$ ),  $z$  is a vertical coordinate (L), positive upwards, and  $t$  is time (T). Equation [3.6.2-1] can be solved nu-

merically using either the standard approximation of the  $h_m$ -based formulation by replacing  $\partial\theta/\partial t$  by  $C(h_m)\partial h_m/\partial t$ , where  $C(h_m) = d\theta/dh_m$  denotes the water capacity function ( $L^{-1}$ ), or the mixed formulation represented by Eq. [3.6.2–1] (Celia et al., 1990). Although Eq. [3.6.2–1] is generally accepted, its derivation for unsaturated macroscopic water flow, including the formulation of the effective hydraulic properties, [i.e., the soil water retention function,  $\theta(h_m)$ , and unsaturated hydraulic conductivity function,  $K(h_m)$ ], includes many assumptions. Most importantly these are:

1. Flow is isothermal, thereby neglecting possible temperature effects on the soil hydraulic properties and temperature-induced water flow.
2. The influence of the air phase on water flow is negligible.
3. The relation between water content and water energy status for a monotonic drainage or wetting process is unique, that is, independent of the water flow rate.

These assumptions are not necessarily fulfilled for transient experiments employed in inverse modeling. Therefore, if deemed appropriate, other flow models may be substituted for Eq. [3.6.2–1]. For example, this was demonstrated by Schultze et al. (1999) and Chen et al. (1999), who used two-fluid phase flow models to simulate unsaturated water flow. To further elaborate on the consequences of these assumptions for simulated water flow is beyond the scope of this study, and we refer the reader to Bear (1972), Nielsen et al. (1986), Quintard and Whitaker (1999), and van Genuchten and Sudicky (1999) for an in-depth analysis.

Some of the presented experimental methods require numerical solution of the two-dimensional flow equation, which for radially symmetric Darcian flow is assumed to be described by:

$$\partial\theta/\partial t = (1/r)(\partial/\partial r)[rK(\partial h_m/\partial r)] + (\partial/\partial z)[K(\partial h_m/\partial z)] + (\partial K/\partial z) \quad [3.6.2-2]$$

where  $r$  is the radial coordinate (L). The applications of Eq. [3.6.2–2], presented below, assume that the soil is uniform and isotropic, and that a multidimensional approach of the problem is required to allow for spatially variable boundary conditions. Otherwise, the same assumptions as for Eq. [3.6.2–1] are applicable.

The soil water retention curve and unsaturated hydraulic conductivity function can be described by various expressions, as presented in Section 3.3.4. However, for convenience, here we use the soil water retention function of van Genuchten (1980)

$$S_e(h_m) = (\theta - \theta_r)/(\theta_s - \theta_r) = 1/(1 + |\alpha h_m|^n)^m \quad [3.6.2-3]$$

which after substitution in the capillary model of Mualem (1976) yields the following hydraulic conductivity model

$$K(h_m) = K_s S_e^l [1 - (1 - S_e^{1/m})^m]^2 \quad [3.6.2-4]$$

In Eq. [3.6.2–3] and [3.6.2–4],  $\theta_r$  and  $\theta_s$  denote the residual and saturated volumetric water contents ( $L^3 L^{-3}$ ), respectively;  $S_e$  is the effective saturation,  $K_s$  is the saturated hydraulic conductivity ( $L T^{-1}$ ),  $l$  is a pore connectivity coefficient, and  $\alpha$  ( $L^{-1}$ ),

$n$ , and  $m = 1 - 1/n$  are empirical coefficients. Most hydraulic models assume that the predictive  $K(\theta)$  is coupled with soil water retention relations through the use of common parameters, as in Eq. [3.6.2–4]. However, the general inverse modeling approach does not require the coupling of the two soil hydraulic functions, and recent studies suggest that improved parameter optimization results are obtained by their decoupling (Vogel et al., 1999; Durner et al., 1999a). Moreover, it has been shown that increased flexibility in the representation of the soil water retention curve, for example, by using a bimodal pore-size distribution model (Durner, 1994; Zurmühl & Durner, 1998) or spline functions (Kulkarni et al., 1998), may improve parameter optimization results. Typically, the number of parameters needed to describe the soil hydraulic functions varies between four and seven. Some parameters can be measured independently (e.g.,  $\theta_s$ ), assigned an assumed value (e.g., the tortuosity parameter,  $l$ ), or related, such as  $n$  and  $m$  in the van Genuchten (1980) expression.

### 3.6.2.2.b Parameter Optimization

**Objective Function—How Can the Optimal Parameter Combination Be Determined?** The following is a summary of the various analyses that are routinely used in the theory and application of inverse modeling. For a more in-depth treatise, we refer the reader to Hopmans and Šimůnek (1999) and Section 1.7.

Desired hydraulic parameters are determined by systematically minimizing the differences between observed and simulated state variables. The total of these differences is expressed by an objective function,  $\phi$ , which may be defined as

$$\phi(\boldsymbol{\beta}, y) = \sum_{j=1}^{j=m_y} v_j \sum_{i=1}^{i=n_j} w_{i,j} [y_j^*(z, t_i) - y_j(z, t_i, \boldsymbol{\beta})]^2 \quad [3.6.2-5]$$

where the right-hand side represents the residuals between the measured ( $y_j^*$ ) and corresponding model-predicted ( $y_j$ ) space–time variables using the soil hydraulic parameters of the optimized parameter vector,  $\boldsymbol{\beta}$ . The first summation sign sums the residual for all measurement types  $m_y$ , whereas the variable  $n_j$  in the second summation denotes the number of measurements for a certain measurement type  $j$ . Typically, in water flow studies,  $y_j^*$  may represent water flux density, cumulative water flow, soil water matric head, or soil water content values. Assuming that the measurement errors within a measurement type are independent and uncorrelated, a weighted least-squares problem represents the maximum likelihood estimator (Section 1.7). Weighting factor values for  $v_j$  can be selected such that data types are weighted equally using a normalization procedure or such that they are equal to the reciprocal of the measurement variance of measurement type  $j$  (Section 1.7); additional weighting ( $w_{i,j}$ ) can be assigned to individual data (Hollenbeck et al., 2000). In addition to the transient measurements, the objective function can also include independently measured soil water retention or unsaturated hydraulic conductivity data points.

Among the various nonlinear optimization techniques available to minimize the objective function (Section 1.7), the Levenberg–Marquardt method is the most

widely used. This method combines the Newton method with the steepest descend method, providing confidence intervals for the optimized parameters.

**Ill-Posedness—Can an Optimum Solution Be Found?** A solution of the inverse problem is attained by minimization of Eq. [3.6.2–5]. To determine whether the inverse problem is at all solvable, it must be “correctly posed”. An incorrectly posed, or *ill-posed*, inverse solution causes nonuniqueness or divergent results. It is generally characterized by nonuniqueness, and/or nonidentifiability, and/or instability of the identified parameters. Instability stems from the fact that small errors in the measured variable may result in large changes of the optimized parameters. Nonuniqueness occurs when a given response leads to more than one set of optimized parameters,  $\beta$ . Generally, the degree of nonuniqueness will increase with an increase in measurement errors of the measured data in  $\phi$ . Nonidentifiability occurs if more than a single parameter set leads to the same model response. If a parameter set is nonidentifiable, the problem is certainly nonunique and therefore ill-posed. Identifiability can be increased, and hence nonuniqueness reduced, by decreasing the number of parameters to be optimized. Nonuniqueness can also be caused by a lack of sensitivity of the flow variables to certain parameter combinations. Accordingly, nonuniqueness depends on the type of measured data, applied values of the weighting factors in Eq. [3.6.2–5], and the suitability of the boundary conditions for the specific flow experiment. Moreover, sensitivity is influenced by the type and number of optimized parameters, and by model and input measurement errors. An experiment must be designed such that direct information is available for the least sensitive parameters, thereby eliminating them from the parameter set, and by providing well-constrained initial estimates. It is generally recommended to test for nonuniqueness by solving the inverse problem repeatedly using different initial parameter estimates.

**Response Surface Analysis—How to Visualize Uniqueness of a Solution?** The behavior of the inverse problem can be evaluated by plotting the value of the objective function ( $\phi$ ), against pairs of optimized parameters to obtain response surfaces. Each response surface is obtained by solving the flow equation, with the appropriate boundary and initial conditions, for many possible combinations of a selected pair of parameter values within a predetermined range, while keeping the other parameters constant. This type of analysis should also be done before the experiment is conducted to investigate the well-posedness of the inverse problem. Since the influence of only two parameters on  $\phi$  is shown in a response surface, each surface represents only a cross section of the full parameter space. The behavior of  $\phi$  across the complete parameter space requires calculating response surfaces for all possible pairs of parameter combinations. Since only two parameters appear within a single response surface analysis, the behavior of  $\phi$  in the various parameter planes is only an indication of the uniqueness of the solution in the full parameter space. For example, local minima may be present, but not appear in any of the cross-sectional planes (Šimůnek & van Genuchten, 1996). On the other hand, response surfaces can reveal the occurrence of local minima, the presence of a well-defined global minimum, and can assist in evaluating parameter sensitivity and correlation. Since the shape of the response surfaces will depend on the measured variables and

the applied experimental boundary conditions, response surface analysis is essential in the evaluation of optimal experimental designs.

**Parameter Uncertainty—How Precise Are the Parameter Estimates?** The precision of the estimated parameters can be assessed by uncertainty analysis, which yields confidence intervals for the estimated parameters at the  $\phi$  minimum. This analysis assumes that uncertainty is caused by measurement errors only, that is, that the model error is zero, and that the inverse solution has converged to the global minimum. Under these conditions, the residuals in  $\phi$  are independent and normally distributed. Uncertainty analysis further assumes that any variable,  $y_j$ , in Eq. [3.6.2–5] is a linear function of the optimized parameters within their computed confidence interval. Although restrictive and only approximately valid for nonlinear problems, the uncertainty analysis provides a means to compare confidence intervals among parameters; thereby indicating which parameters should be measured or estimated independently. For the stated assumptions, parameter standard deviation values can be determined and confidence intervals can be estimated. However, these confidence interval estimates are not necessarily correct if parameters are correlated. In addition, correlated parameters can cause a slow convergence rate, and will increase nonuniqueness and parameter uncertainty. Hollenbeck et al. (2000) pointed out that testing of the hydraulic model's adequacy is required first before parameter uncertainty analysis is conducted. Clearly, uncertainty analysis of optimized hydraulic parameters is not meaningful if the tested model fails the adequacy test, for example, because of experimental or modeling errors. For that purpose, a correlation analysis between measured and optimized flow variables only is not sufficient, but should include a residual analysis, obtained from a plot of observed and simulated data vs. the independent variable (space and/or time). Model adequacy can be tested statistically by comparing the average residual with a predefined (expected) measurement error, as estimated from experience or sensor specifications. In Eq. [3.6.2–5], inadequate hydraulic models yield  $\phi$  values that are larger than one, if  $v_j = 1/n_j\sigma_j^2$  ( $\sigma_j^2$  is measurement error variance) and  $w_{i,j} = 1$ .

**Sensitivity Analysis—Is the Experimental Design Suitable?** Parameter sensitivity is determined by the derivative of the objective function with respect to a particular parameter. A flow experiment designed for inverse modeling should include measurements that are most sensitive to changes in the optimized parameters, thereby eliminating ill-posedness. The sensitivity analysis of the optimization problem depends on type, location, and frequency of measurements; thereby providing information on the optimal experimental design. Moreover, a higher sensitivity will result in quicker convergence of the parameter estimation problem. Sensitivity coefficients can be computed a priori from hypothetical experiments, using the Jacobian, as defined in Eq. [1.7–15] and [1.7–17] in Section 1.7. Large sensitivity values indicate a well-defined minimum with precise parameter estimates. Sensitivity and parameter uncertainty are inversely related; that is, highly sensitive measurement variables yield small parameter uncertainties for a given measurement error. Since the Jacobian matrix is determined for the optimum parameter set only, the sensitivity coefficients characterize the behavior of  $\phi$  at its minimum, and do not describe problem sensitivity anywhere else in the parameter space. Sensitivity coefficients can be calculated as a function of time (Inoue et al., 1998), and can be

used to determine optimum sensor location within the spatial domain of the experiment. Moreover, as was reported by Zurmühl and Durner (1998), a similar shape of plots with parameter sensitivity coefficient vs. time indicates correlated parameters.

In summary, it must be pointed out that the success of inverse modeling depends on the suitability and quality of each of the three earlier mentioned components, namely, (i) the experimental design, that is, the choice of boundary conditions, the location and time resolution of the measurement sensors, and the degree of accuracy of the experimental data; (ii) the suitability of the transient flow model and hydraulic functions; and (iii) the robustness of the optimization algorithm as determined by its convergence to a global minimum. If any of these three components is unsatisfactory, inverse modeling may diverge (fail to find a global minimum), or result in an ill-posed problem yielding inaccurate parameters with high uncertainties. Further requirements for well-posed problems will be illustrated in the example in Section 3.6.2–8.

### 3.6.2.3 Multistep Outflow Method

#### 3.6.2.3.a Introduction

Kool et al. (1985) were among the first to apply the inverse approach by numerical solution of the Richards equation for a one-step outflow experiment. They concluded that uniqueness problems are minimized if the experiment is designed to cover a wide water content range. Moreover, they also determined that initial parameter estimates must be reasonably close to their true values and that outflow measurement errors must be small. Parker et al. (1985) subsequently experimentally applied the one-step method to four different soils of different texture and concluded that  $\theta(h_m)$  and  $K(\theta)$  can be optimized simultaneously by using cumulative outflow as a function of time. It was also found that the optimized soil hydraulic functions could be extrapolated to a water content range beyond that achieved with the single pressure step by including in the objective function an independently measured point on the soil water retention curve.

The need for independently measured soil water retention data in the one-step outflow optimization procedure was demonstrated by van Dam et al. (1992). In their study, measured unsaturated hydraulic conductivity data were compared with optimized hydraulic functions using the one-step outflow procedure with and without measured  $\theta(h_m)$  data. They concluded that optimization using measured outflow data alone is inadequate and that additional retention data are necessary to obtain accurate  $K(\theta)$  functions. Similarly, Toorman et al. (1992) concluded that uniqueness problems in the transient one-step outflow experiment were minimized if matric head data were included in the objective function.

To circumvent the need for additional soil water pressure measurements in the outflow experiment, van Dam et al. (1994) conducted outflow experiments in which the pneumatic pressure was increased in several smaller steps. Their work, using a loam soil, showed that the outflow data of a multistep experiment contained sufficient information for unique estimates of the soil hydraulic functions. The experimental work by Eching and Hopmans (1993a, b) and Eching et al. (1994) showed how the multistep method, when combined with automated matric head

measurements during drainage of the soil core, resulted in unique parameter values for the optimized soil hydraulic functions for four different textured soils. In their analysis, an excellent match between optimized and independently measured soil water retention and unsaturated hydraulic conductivity data was found. The multistep outflow method was also recommended by Durner et al. (1999b) after they compared it with the classical one-step method, although they also showed that the performance of the one-step method depends largely on the pressure step size relative to the shape of the soil water retention function. Their work further demonstrated that a reliable estimation of the unsaturated hydraulic conductivity function is dependent on the accuracy of the retention model, if the coupled approach of Eq. [3.6.2–4] is used. They concluded that combination of the multistep method with outflow and tensiometric data in the objective function would yield accurate estimations of both the retention and the hydraulic conductivity parameters for a wide range of soil textures.

### 3.6.2.3.b Experimental Procedures

The experimental apparatus (Fig. 3.6.2–2) is based on the pressure cell method, presented in Section 3.3.2, and can be adapted (Eching et al., 1993b) to include one or two miniature tensiometers connected to pressure transducers (Wildenschild et al., 2001). The porous membrane can be either a ceramic plate or porous nylon (MSI Inc., Westborough, MA) with a sufficiently high air-entry value. The advantage of the porous nylon is its low resistance, thereby minimizing pressure differences across the membrane. However, the thin membrane accelerates the possible diffusion of soil gas across the membrane, thereby causing accumulation of gas beneath the membrane. Gas accumulation, caused by exsolution of air from the water phase can be eliminated by using pressurized  $N_2$  gas instead of air. Continuous and unattended monitoring of drainage flow rates can be easily accomplished by installation of a pressure transducer in the bottom of a water-receiving burette. Details of various experimental setups can be found in Eching and Hopmans (1993a, b) and Zurmühl (1998).

After assembling the soil core between the end plates and insertion of the tensiometer(s), the soil is saturated with a  $CaCl_2$  solution (0.0001–0.01  $M$ , depending on soil type and Na content). If needed,  $AgNO_3$  solution, mercuric chloride and/or thymol (see Section 3.3.2.1.d) should be added to the saturating solution to prevent microbial clogging of the porous membrane and/or soil pores. After saturation, the pressure transducers can be calibrated from known pressures in the soil water and the burette. Subsequently, the soil is slightly unsaturated by exceeding its air-entry value across to height of the sample to assure the presence of a continuous gas phase at the start of the multistep experiment. As was demonstrated by Hopmans et al. (1992), this is needed to obtain a correct solution of the Richards equation, by ensuring the availability of air to displace the water phase during the drainage experiment.

After hydraulic equilibrium has been established, the first pressure increment is applied and the soil matric head and drainage volume are continuously monitored and logged using the pressure transducers. The volumetric water content at the conclusion of the outflow experiment is determined by oven-drying the soil core. Sat-

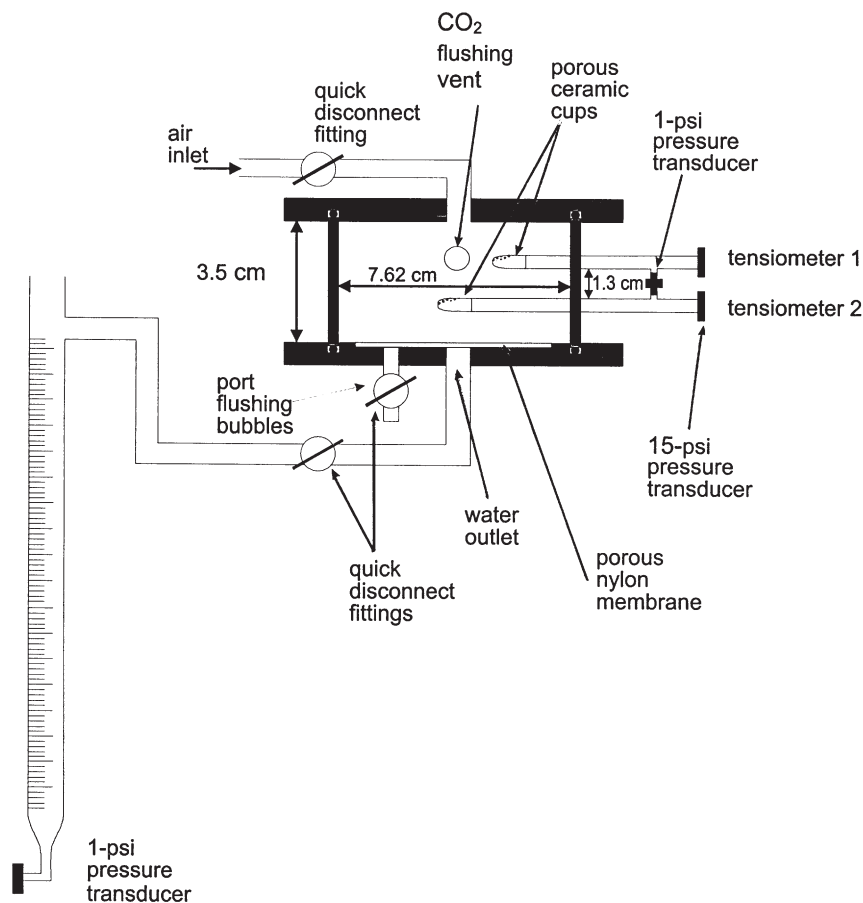


Fig. 3.6.2-2. Schematic of the apparatus for outflow experiments (modified from Wildenschild et al., 2001).

urated and initial water content values, in addition to intermediate volumetric water content values, are back calculated using this oven-dry value and the measured cumulative outflow volumes between pressure steps. The multistep outflow technique will be improved by including the following considerations:

1. The choice of the number and magnitude of the pressure increments is not known a priori. In the limiting case, one may select a single pressure increment (one-step outflow experiment). However, it has been clearly demonstrated that selection of multiple steps increases the sensitivity of the measurements with regard to the parameters to be optimized. We recommend using available information on soil water retention to select the number and size of the pressure increments, thereby making sure that the general shape of the retention curve is preserved. This means that pressure differences should be small near the air-entry point, where the retention curve is steep, but can be large for the dry range, where the retention curve is

Tables 3.6.2–1. Thickness ( $d$ ), saturated hydraulic conductivity ( $K_s$ ), resistance ( $R$ ), and air-entry pressure ( $h_{a,e}$ ) for a ceramic plate, sintered glass plates (Robu, Hattingen, Germany), and a nylon membrane (Osmonics Laboratory Products; www.osmolabstore.com).

	$d$	$K_s$	$R$	$h_{a,e}$
	cm	cm h <sup>-1</sup>	h	kPa
Ceramic plate	0.74	0.0498	14.86	100
Sintered glass plate P5	0.70	0.1	7	45
Sintered glass plate P4	0.70	2.1	0.33	15
Sintered glass plate P3	0.70	8.5	0.08	7
Nylon membrane	0.01	0.025	0.4	170

nearly flat. Ideally, one selects the pressure increments such that about equal drainage volumes are obtained for each increment.

2. Questions are often asked about the duration of pressure increments. There are various issues that must be considered. First, it has been shown (e.g., Schultze et al., 1999) that one of the most important advantages of the inverse method is that excellent results can be obtained without waiting for hydraulic equilibrium between pressure steps. Moreover, true hydraulic equilibrium is often not attained in the dry soil moisture range, because of the low unsaturated hydraulic conductivity value of the soil core, especially near the porous membrane. As the duration of the outflow experiment increases, there is increasing danger of air accumulation under the porous membrane by gaseous diffusion and clogging of the membrane and soil by microbial growth. If no tensiometric measurements are taken, however, one might prefer increasing the gas pressure only after there is no measurable outflow, which makes the method equivalent to the one presented in Section 3.3.2.

3. To increase the sensitivity of the parameter optimization procedure, it is important to minimize the influence of the porous membrane on drainage rate. For example, the resistance of the porous membrane must be low relative to that of the unsaturated soil. This might not be the case when using thick porous ceramic plates for near-saturated, coarse-textured soils. Therefore, it is recommended to use a thin nylon porous membrane with a large air-entry value (Table 3.6.2–1). The low resistance nylon membrane creates only minor differences in water pressure across the membrane, and is now routinely used in outflow experiments. Moreover, the low resistance nylon membrane eliminates the need for a separate calculation of the matric head at the soil–membrane interface for direct conductivity calculations. However, care must be taken to maintain hydraulic contact between the membrane and the soil sample. Especially for sandy soils, highly conductive sintered glass plates with limited air-entry pressures are a viable alternative (Table 3.6.2–1). If the resistance of the porous plate or nylon membrane is not negligible, it must be included in the numerical simulation of the experiment, effectively requiring simulation for a two-layered domain. Under these circumstances, the porous membrane in the flow domain must be replaced by an equivalent porous medium with the same total resistance. In any case, it is good practice to measure the plate resistance or its saturated hydraulic conductivity separately, before and after the experiment, to assess whether clogging has occurred due to microbial growth or migration of soil particles.

4. A well-posed inverse problem is achieved if the matric head is measured in the soil core during the outflow experiment. A single tensiometer is best placed

near the center of the soil core. However, insertion of a second tensiometer close to the bottom outflow boundary is recommended, since it provides valuable information about the validity of the pressure continuity assumption across the porous membrane.

5. In the dry range, it is often found that, although outflow has essentially ceased, the soil water matric head is not in equilibrium with the water beneath the porous membrane. That is, at low water content values, the corresponding hydraulic conductivity values are too low for drainage to occur, thereby preventing the soil from attaining hydraulic equilibrium. This is especially the case for coarse-textured soils and has wide implications for soil water retention measurements in general (see Section 3.3.1).

6. As static equilibrium conditions are not required in the inverse analysis, there is additional freedom in the selection of the physical dimensions of the soil core. However, column length affects parameter sensitivity in two ways. It is expected that the sensitivity for the hydraulic conductivity parameters increases with increasing core length because of the resulting increasing flow rates. Alternatively, the sensitivity of the soil water retention parameters increases as the soil core length decreases. The practical core length ranges from 5 to 20 cm. The core diameter has no effect on parameter sensitivity; however, collection of larger-diameter cores reduces among-core variability in undisturbed soils.

7. The general recommendation to start a transient outflow experiment at near saturation by exceeding the soil's air-entry value first will reduce the sensitivity of the saturated hydraulic conductivity on the inverse solution. Moreover, an initial drainage experiment on the same core is required to define the soil's air-entry value. The near-saturation requirement is not needed if the initial pressure step, starting from saturation, is slightly larger than the air-entry value of the soil.

### 3.6.2.3.c Simulations and Optimization

Initial and boundary conditions applicable to the multistep experiment are

$$\begin{aligned} h_m(z,t) &= h_{m,i}(z) & t = 0, 0 < z < L \\ q(z,t) &= 0 & t > 0, z = L \\ h_m(z,t) &= h(z,t) - h_a & t > 0, z = 0 \end{aligned} \quad [3.6.2-6]$$

where  $h_{m,i}$  is the initial matric head,  $q$  denotes the flux density ( $L T^{-1}$ ),  $z = 0$  is the bottom of the porous membrane or plate,  $z = L$  is the top of the soil core,  $h(0,t)$  is the water pressure head at the bottom of the porous membrane, and  $h_a$  is either the pneumatic gas pressure applied to the top of the soil core ( $z = L$ ) or the suction applied beneath the porous membrane ( $z = 0$ ). For example, if  $h(0,t) = 1$  cm (height of water above the bottom of the porous membrane), and  $h_a = 80$  cm (applied to the top of the soil core), then  $h_m = -79$  cm. Similarly, for the same water level in the burette, if an 80-cm suction head is applied to the water in the burette,  $h_m = -79$  cm. The objective function, Eq. [3.6.2-5], includes the matric head measurements inside the soil core ( $j = 1$ ) and cumulative drainage volume ( $j = 2$ ) vs. time. It is rec-

ommended to select a relatively small time interval between measurements (input to data logger), and to smooth and eliminate data later, rather than selecting the number of required measurements ( $n_j$ ) a priori. Additional comments that provide guidance towards successful application of the multistep outflow method are:

1. Although the limitations with respect to the experiment or flow modeling are few, the inverse approach relies on the availability of a universally applicable nonlinear optimization algorithm. Problems with the parameter optimization technique generally are associated with the difficulty of defining an objective function that will yield unique and convergent solutions. Since ill-posedness of the inverse problem can be caused by correlation between the parameters to be optimized, uniqueness of the optimized parameters is generally increased by reducing the number of free parameters. For example, if parameter values can be measured independently, their values should be fixed or be included in the objective function as Bayesian estimates (Section 1.7). To further reduce the number of parameters to be optimized, we often make use of the relationship between  $m$  and  $n$  ( $m = 1 - 1/n$ ) and couple the retention curve model with the conductivity curve model (van Genuchten, 1980). Furthermore, the tortuosity parameter of the conductivity function,  $l$ , is frequently set to a fixed value ( $l = 0.5$  according to Mualem, 1976;  $l = -1$  according to Schaap & Leij, 2000).

2. Because the Richards equation includes the soil water retention function,  $\theta(h_m)$ , only by way of its derivative,  $\partial\theta/\partial t = C(h_m)\partial h_m/\partial t$ , where  $C(h_m) = d\theta/dh_m$ , the residual and saturated water contents ( $\theta_r$  and  $\theta_s$ ) are perfectly correlated. Consequently, only one of these two parameters may be optimized. In practice,  $\theta_s$  is independently measured from oven-drying at the conclusion of the outflow experiment. The parameters  $\theta_r$  and  $\theta_s$  can be estimated simultaneously only if some additional water content-related information is included in the optimization (e.g., the initial condition is given in terms of water content; the initial or final water volume in the sample is included into the objective function).

3. It must be stressed that uniqueness of the coupled retention and conductivity solution will depend on the selection of the hydraulic models and their ability to accurately represent the true soil hydraulic properties. For example, Zurmühl and Durner (1998) and Durner et al. (1999a) demonstrated that optimization with eight or more fitting parameters was stable and unique if bimodal hydraulic models were used for soils with a bimodal pore-size distributions. Furthermore, a non-suitable retention function can lead to a meaningless estimate of the conductivity parameter,  $l$  (Durner et al., 1999b).

4. Extrapolation beyond the range of measurement is associated with a high level of uncertainty. To increase the range of validity of the optimized hydraulic functions, it is recommended to include independently measured soil water retention and/or conductivity data in the objective function. For example, with the experimental range limited by the largest applied pressure, soil water retention points at lower matric head values, as measured with the pressure plate extractor (Section 3.3.2.4) or the evaporation method (Section 3.6.2.4), may be included to augment the water content range of the optimized hydraulic functions.

5. Outflow methods provide few dynamic data at near saturation. This implies that the sensitivity of the method to the shape of the conductivity function near

saturation, and in particular the sensitivity for estimating the saturated conductivity parameter,  $K_s$ , is low. Nevertheless, it is frequently recommended not to fix  $K_s$  at the value of an independently measured saturated conductivity (Section 3.4) but to treat it as an empirical fitting parameter because this often improves the description of the overall conductivity function, particularly for undisturbed soils. However, disagreement between fitted and measured  $K_s$  may indicate that the shape of the assumed parametric form of the conductivity function near saturation might not be correct (Durner, 1994).

6. As was demonstrated by Eching and Hopmans (1993a), the multistep outflow experiment can be extended to optimize soil hydraulic parameters for soil wetting by reversing the time sequence of the pressure increments starting with an initially dry soil. Hence, combined analysis of a drying experiment followed by a wetting experiment allows simultaneous optimization of hysteresis (Schultze et al., 1996; Zurmühl, 1998). However, as reported by Durner et al. (1999b), poor agreements between optimization results and independent measurements might occur if an incorrect hysteresis model is used.

7. Recently, the choice of appropriate weighting factors in the objective function, Eq. [3.6.2–5], has been put into question, especially with regard to the calculations of the uncertainty of the optimized parameters. A poor choice of the measurement error can result in either too narrow or extremely large confidence intervals (Hollenbeck & Jensen, 1998a), thereby leading to incorrect interpretations of the optimization results. Using a parameter sensitivity analysis, Vrugt et al. (2001b) showed that uniqueness of a multistep outflow experiment without matric head measurements can be significantly improved by including in the objective function only the outflow measurements immediately following the applied pressure increments, when flow rates are highest, in addition to the total outflow at the end of each pressure step.

8. The ability of estimating soil hydraulic functions using inverse procedures has raised the question whether hydraulic properties might be influenced by the flow rate or boundary conditions. The effect of the flow dynamics can be caused by water entrapment or by discontinuity of water-filled pores for large matric head gradients (see Section 3.3.1). Research is ongoing (Wildenschild et al., 2001; Mortensen et al., 1998) to investigate these dynamic effects. Additional complications were reported by Hollenbeck and Jensen (1998b), who addressed the difficulty of experimental reproducibility, and Schultze et al. (1999), who cautioned that outflow experiments might include air-phase effects that should be incorporated by two-phase flow modeling instead of describing water flow by the traditional Richards equation (Eq. [3.6.2–1]) only.

9. Some have expressed concerns about the step-wise changes of the boundary condition, which may cause a flow behavior that does not occur in nature (van Dam et al., 1994). As an alternative to the multistep method, a continuous outflow method was tested using a gradual change of the pressure boundary condition. Durner et al. (1999b) discussed the comparison of the multistep outflow method with this continuous method. They concluded that the two methodologies are equally suitable for identifying the water retention parameters. However, the small flux rates reduced the sensitivity of the hydraulic conductivity, thereby making the continuous outflow method less suitable.

10. Finally, measured drainage rate and matric head data can also be used to estimate the unsaturated hydraulic conductivity data directly. The concepts of the direct hydraulic conductivity estimation were discussed by Eching et al. (1994) and Liu et al. (1998). The procedure requires estimation of the matric head at the soil–membrane interface. Since outflow rates are relatively high at the beginning of each pressure step, it is preferred to use data from the time periods immediately following an increase in applied air pressure. If so required, the matric head at the soil–membrane interface is estimated from the saturated hydraulic conductivity and thickness of the saturated porous membrane in combination with known measured values of the water pressure at the bottom of the membrane and the measured drainage rate. The effective permeability of the soil can be estimated subsequently from the Darcy equation solving for  $K(S_e)$ , after substituting the average drainage rate and the assumed  $h_m$  gradient in the soil core using the measured matric head values in the center of the core and at the soil–membrane interface (Wildenschild et al., 2001).

#### 3.6.2.4 Evaporation Method

##### 3.6.2.4.a Introduction

The parameter estimation technique has also been successfully applied to the laboratory evaporation technique (Section 3.6.1.1.c). The evaporation method was first introduced by Gardner and Miklich (1962), who imposed a series of constant evaporation rates to one side of a soil sample after first allowing the sample to attain hydraulic equilibrium before the next evaporation rate was applied. They measured the matric head response of two tensiometers. Becher (1971) simplified the evaporation method by using a constant evaporation rate. Several other modifications of the evaporation method, with simultaneous measurements of evaporation rate and matric head values at different heights in the sample, have since been developed (Wind, 1968; Boels et al., 1978; Schindler, 1980; Tamari et al., 1993; Wendroth et al., 1993; Halbertsma & Veerman, 1994). Experimental data obtained with the evaporation method can be analyzed using either a simple approach introduced by Schindler (1980), the classical Wind analysis or its modifications (e.g., Wind, 1968; Wendroth et al., 1993; Halbertsma & Veerman, 1994), or increasingly more often from numerical inversion (Ciollaro & Romano, 1995; Santini et al., 1995; Šimůnek et al., 1998c, 1999c).

In their review, Feddes et al. (1988) obtained reasonable agreement between hydraulic conductivities determined from parameter estimation by the inverse procedure and using Wind's method (Wind, 1968). As part of a study of the spatial variability of soil hydraulic properties, Ciollaro and Romano (1995) successfully used the inverse procedure to estimate parameter values, based on evaporation experiments, to determine the soil hydraulic parameters of a large number of samples. Santini et al. (1995) also used parameter estimation by the inverse procedure in connection with evaporation experiments. Their results compared favorably with independently measured retention and saturated hydraulic conductivity data. Šimůnek et al. (1998c) obtained excellent correspondence between retention curves and hydraulic conductivity functions obtained with parameter estimation by the inverse technique and the modified Wind's method (Wendroth et al., 1993). They also

showed that, contrary to Wind's method, which requires matric head measurements at several locations, comparable results could be obtained with tensiometer readings at just one location. Romano and Santini (1999) showed that the inversion results compared satisfactorily with soil hydraulic data as measured independently with the instantaneous profile method (Section 3.6.1.2.a). However, they concluded that in some cases unsaturated hydraulic conductivity functions with parameters independent of the soil water retention functions are needed for accurate hydraulic characterization.

#### 3.6.2.4.b Experimental Procedures

Detailed experimental procedures are outlined in Šimůnek et al. (1998c) and Romano and Santini (1999) and will only be summarized here. Initially, saturated 10-cm-high soil cores are placed on a ceramic plate to establish a static initial matric head distribution. Two to five miniature tensiometers are placed horizontally at different vertical locations in the soil core. After tensiometer equilibration, as evidenced from the tensiometer readings, the soil core is placed on an impermeable plate for the evaporation experiment. Total soil water storage changes are determined from weight measurements of the soil core. A strain-gauge load cell placed under the plate bearing the soil sample is used for soil sample weight measurements, while the matric head is monitored at the various soil depths connecting the tensiometers to pressure transducers. Calibrating each transducer across the working pressure range should be performed before and after the test. An evaporation rate can be induced using either natural laboratory conditions, or can be accelerated using a fan to blow air across the sample surface. A two-rate experiment can also be used in order to induce initially sufficiently large matric head gradients (Wendroth et al., 1993). Once the  $h_m$  gradient is about 1.5 to 2.5 m m<sup>-1</sup>, evaporation is allowed to continue without the fan. The experiment is terminated after the matric head values become too low for reliable functioning of the tensiometers.

Additional comments regarding the experimental setup are:

1. Extrapolation beyond the measurement range is associated with a high level of uncertainty. Inclusion of independently measured information beyond the measurement range, that is, additional soil water retention data or a residual water content value, could greatly decrease this uncertainty.

2. Using the inverse modeling approach, it has been shown that matric head readings from a single tensiometer in combination with a final soil water storage measurement may be adequate to guarantee precise estimation of the soil hydraulic characteristics within the range of measurements (Šimůnek et al., 1999c). Maximum sensitivities are generally attained by placing this single tensiometer near the evaporating soil surface where the largest soil water content changes occur. However, tensiometer placement very close to the soil surface is discouraged, as the soil surface remains dry for most of the latter part of the evaporation experiment, so that its information is limited. Moreover, to guarantee sufficient time measurements of changes in matric head, especially when hydraulic head gradients become large or as backup information if a tensiometer fails, at least two tensiometer locations are recommended.

### 3.6.2.4.c Simulation and Optimization

The governing flow equation for one-dimensional isothermal Darcian flow is given by Eq. [3.6.2–1]. Boundary and initial conditions applicable to an evaporation experiment are as follows:

$$\begin{aligned} h_m(z,t) &= h_{m,i}(z) & t = 0, 0 < z \leq L \\ q(z,t) &= q_{\text{evap}}(t) & t > 0, z = L \\ q(z,t) &= 0 & t > 0, z = 0 \end{aligned} \quad [3.6.2-7]$$

where  $q_{\text{evap}}(t)$  is the time-variable evaporation rate ( $L T^{-1}$ ) imposed at the soil surface, and all other variables are as defined in Eq. [3.6.2–6].

The objective function to be minimized includes all matric head measurements and a soil water storage value. This single water storage value provides a water content reference from which the saturated water content can be estimated using the evaporation rate data. The inclusion of more values of water storage in the objective function does not improve the optimization process, since the evaporation rate (upper boundary condition) is always enforced. A sensitivity analysis can be used to determine the optimum tensiometer location for the parameter estimation procedure.

Additional comments include:

1. Parameter sensitivity is not affected by soil core height. However, duration of the evaporation experiment will be less for shorter soil cores. Šimůnek et al. (1999c) analyzed the sensitivity of the parameters of the van Genuchten relationship for a hypothetical two-rate evaporation experiment with tensiometer locations at depths of 1, 3, 5, 7, and 9 cm within a 10-cm-high sample. Their results showed that (i) the sensitivity increased as the experiment progressed in time and the soil core became drier, (ii) the sensitivity was highest for tensiometer 1, closest to the evaporating soil surface, and (iii) the matric head was most sensitive to  $n$  and  $\theta_s$ , whereas the sensitivities of the parameters  $\alpha$ ,  $\theta_r$ , and  $K_s$  were, by comparison, much smaller.

2. While a two-rate evaporation experiment has important advantages over a one-rate experiment when using the modified Wind method, the two-stage approach did not show an advantage in the parameter estimation approach by the inverse method, except that it will speed up the experiment. In addition, it was concluded by Romano and Santini (1999), who used a parameter uncertainty analysis of hypothetical numerical experiments for coarse-textured soils, that smaller parameter confidence intervals were obtained when evaporative fluxes increased.

3. When numerically solving the evaporation process, certain combinations of soil hydraulic parameters, selected by the parameter optimization procedure, may cause physically impossible water delivery rates towards the soil surface to satisfy the required evaporation flux. This may especially occur at the later stages of the evaporation experiment, when water contents near the soil surface are low. To eliminate convergence problems in such situations, the evaporation rate boundary condition must be replaced by a minimum allowable matric head value (about  $-100$  to

–150 m) at the expense of disagreement between simulated and measured evaporation fluxes. Since this will usually result in larger residuals, selected hydraulic parameter values must be adjusted in the subsequent iterations so that imposed evaporation fluxes can be enforced.

4. In principle, the evaporation and the multistep outflow methods represent similar flow processes. In practice, however, there are some important differences. First, the multistep outflow method imposes abrupt step-wise changes of the pressure boundary condition, thereby inducing high flow rates, particularly under wet conditions. In contrast, the evaporation method imposes a smooth change of the boundary condition, which is more typical of a natural drying process. Second, as the soil drains, the outflow rates in the multistep method decrease due to the hydraulic head gradient approaching zero, thereby reducing the sensitivity of the hydraulic parameters. In the evaporation method, however, the hydraulic head gradients increase as the soil dries, thereby gaining parameter sensitivity within the operable range of tensiometric measurements (usually  $h_m > -800$  cm). Consequently, the evaporation method is preferable for hydraulic characterization in the intermediate water content range, whereas the multistep outflow method is recommended for estimation of soil hydraulic functions in the wet range. As stated above, the range of validity can be extended for both methods by including independently measured data in the objective function.

### 3.6.2.5 Tension Disc Infiltrometer

#### 3.6.2.5.a Introduction

Tension disc infiltrometers have recently become very popular devices for in situ measurements of the near-saturated soil hydraulic properties (Perroux & White, 1988; Ankeny et al., 1991; Reynolds & Elrick, 1991; Logsdon et al., 1993). Tension infiltration data have been used primarily for evaluating saturated and unsaturated hydraulic conductivities, and to quantify the effects of macropores and preferential flow paths on infiltration. Tension infiltration data are generally used to evaluate the saturated hydraulic conductivity,  $K_s$ , and the sorptivity parameter in Gardner's (1958) exponential model of the unsaturated hydraulic conductivity using Wooding's (1968) analytical solution (see Section 3.5.4). Adequate parameter estimation requires either infiltration measurements using two different disc diameters (Smettem & Clothier, 1989), or infiltration measurements using a single disc diameter but multiple tensions (e.g., Ankeny et al., 1991).

Although early-time infiltration data from the tension disc infiltrometer can be used to estimate the sorptivity (White & Sully, 1987) and the matrix flux potential, only steady-state infiltration rates are usually used for Wooding-type analyses. Šimůnek and van Genuchten (1996, 1997) suggested using the entire cumulative infiltration curve in combination with parameter estimation to estimate additional soil hydraulic parameters. From an analysis of numerically generated data for one supply tension experiment they concluded that the cumulative infiltration curve by itself does not contain enough information to provide a unique inverse solution. Hence, additional information about the flow process, such as the water content and/or matric head measured at one or more locations in the soil profile is needed to successfully obtain unique inverse solutions for the soil hydraulic functions.

### 3.6.2.5.b Experimental Procedures

Details of the experimental procedure are outlined in Section 3.5.4. Usually, the soil surface is covered with a thin layer of sand to ensure hydraulic contact between the disc and the underlying soil. The sand should have a sufficiently large air-entry value to remain saturated at all applied tensions. It should also have a  $K_s$  value that is large enough to prevent extensive flow impedance effects (Reynolds & Zebchuk, 1996). The disc is connected with a tension-controlled water supply system, and transient infiltration rates can be accurately determined from pressure transducers connected to a data logging system (Ankeny et al., 1988). Water is supplied initially at the greatest suction and is decreased consecutively to a lower suction each time steady state has been attained. If desired, time domain reflectometry (TDR) or tensiometers can be installed below the supply disc to monitor water content and/or matric head changes (Wang et al, 1998; Šimůnek et al., 1999d). Alternatively, soil samples can be taken before and after an experiment (near and below the supply disc) and be used for initial and final volumetric water content determinations.

Šimůnek and van Genuchten (1997) studied infiltration at several consecutive supply tensions. They considered several scenarios with different levels of information and concluded that the most practical experiment for inverse estimation of the hydraulic parameters is the cumulative infiltration curve measured at several consecutive tensions, augmented with the initial and final water content values directly below the disc.

### 3.6.2.5.c Simulation and Optimization

Simulation of flow from the tension disc infiltrometer requires use of the radially symmetric two-dimensional flow equation (Eq. [3.6.2–2]) The following initial and boundary conditions apply

$$\begin{aligned}
 \theta(r,z,t) &= \theta_i & t = 0, 0 < r < \infty, 0 < z < \infty \\
 h_m(r,z,t) &= h_{m,o}(t) & t > 0, 0 < r < r_o, z = 0 \\
 q(r,z,t) &= 0 & t > 0, r > r_o, z = 0 \\
 h_m(r,z,t) &= h_{m,i} & t > 0, r \rightarrow \infty, z \rightarrow \infty
 \end{aligned} \tag{3.6.2–8}$$

where  $\theta_i$  and  $h_{m,i}$  denote constant initial water content and matric head (at zero time and far away from the infiltration source), respectively,  $r_o$  is the infiltration disc radius (L), and  $h_{m,o}$  is the time-variable water supply pressure at the infiltrometer membrane (L). Flow symmetry is assumed around the  $r = 0$  axis, which is therefore also a no-radial-flux boundary.

The objective function defined in Eq. [3.6.2–5] includes cumulative infiltration data for the successively supplied water pressures, and may include additional information such as matric head and/or water content data below the supply disc at various  $(r,z)$  positions as a function of time. In addition, the objective function could include a Bayesian estimate (Section 1.7) of the unsaturated hydraulic con-

ductivity computed from Wooding's (1968) analysis. We provide the following additional comments:

1. The inverse method was tested by Šimůnek et al. (1998a) using data collected as part of the soil hydrology program of the HAPEX-Sahel regional-scale experiment (Cuenca et al., 1997). A tension disc diameter of 25 cm with supply tensions of 11.5, 9, 6, 3, 1, and 0.1 cm was used. Agreement between the measured and optimized cumulative infiltration curves was very good. The inverse method and Wooding's (1968) analysis gave almost identical unsaturated hydraulic conductivities for matric head values in the interval between  $-2$  and  $-10.25$  cm. However, the hydraulic conductivity in the highest-matric head range (between  $-1$  and  $-0.1$  cm) was overestimated by a factor of two using Wooding's analysis.

2. The Šimůnek et al. (1998a) results also suggest that tension disc experiments may provide adequate information to estimate both the unsaturated hydraulic conductivity and the soil water retention properties, and that there is no need for additional tensiometer and TDR measurements to better define the inverse problem. Parameters of the soil water retention curve can be closely coupled with those of the unsaturated hydraulic conductivity function, as is the case with the van Genuchten–Mualem model. The fitting of the cumulative infiltration curves was improved by allowing the pore-connectivity parameter to be optimized as well, rather than assuming a constant value of  $l = 0.5$ .

3. The public domain program DISC (Šimůnek & van Genuchten, 2000) for analyzing tension disc infiltrometer data to estimate parameter values by the inverse procedure is available from the U.S. Salinity Laboratory, Riverside, CA (<http://www.usssl.ars.usda.gov>) and from Soil Measurement Systems, Tucson, AZ.

### 3.6.2.6 Field Drainage

#### 3.6.2.6.a Introduction

Certainly the most popular experiment to determine the soil water retention and hydraulic conductivity functions in the field (in situ) has been the instantaneous profile method (Hillel et al., 1972; Vachaud et al., 1978; Section 3.6.1.2.a). The first application of a parameter optimization technique to instantaneous profile field data was carried out by Dane and Hruska (1983). These authors questioned the uniqueness of the solution and concluded that the sensitivity of the optimized parameters depended on the prescribed boundary conditions. Kool et al. (1987) performed a successful inversion using lysimeter data and a slightly different approach than Dane and Hruska (1983). Kool and Parker (1988) investigated the numerical inversion of hypothetical in situ infiltration and redistribution flow events and showed the advantages of including simultaneous measurements of pressure heads and water contents in the optimization procedure.

Santini and Romano (1992) provided guidelines for an optimal design of the field drainage experiment and explored the feasibility of simplifying the experimental procedures while maintaining acceptable parameter uncertainty. For example, they proposed reducing the number of  $\theta$  and  $h_m$  measurements within a vertical soil profile. To overcome limitations regarding the lower boundary condition, Romano (1993) investigated the effectiveness of defining a fixed hydraulic head gra-

dient and the possibility of including it as an additional optimization parameter value. However, this approach may not apply to layered soils. Zijlstra and Dane (1996) applied the parameter optimization technique to layered soils, and concluded that the inverse problem may become ill-posed because of the increased number of optimized parameters. Their soil profiles consisted of one, two, or three distinct horizons, and they used water content measurements as a function of time and depth, and matric head values as a function of time at the bottom boundary, to minimize the objective function. The ill-posedness of the inverse problem depended on the size of the input data set.

#### 3.6.2.6.b Experimental Procedures

Parameter estimation of unsaturated soil hydraulic properties from an in situ transient drainage experiment involves soil water content and matric head measurements at multiple times and soil depths. The field setup is basically the same as for the classic instantaneous profile method (Section 3.6.1.2.a), but some simplifications are possible and will be discussed.

First, a profile description is needed to determine the major horizon boundaries. The experiment should be conducted on a leveled, vegetation-free plot with an area not smaller than 12 m<sup>2</sup>. The plot should be instrumented in the center with measurement sensors located at depths depending on the soil profile description. The experiment is initiated by ponding water over the entire plot area until matric head values are approximately zero or do not change with time at any of the depth locations. After the water supply is stopped and the ponded water has infiltrated, the plot is covered with a plastic sheet and insulated to ensure a zero-flux top boundary condition and to reduce temperature variations. Subsequently, the soil is allowed to drain by gravity. The transient drainage process is monitored by simultaneous measurements of soil water content and matric head until no changes with time occur. Tensiometers are usually installed at 15-cm depth increments with at least one tensiometer in each soil horizon. Volumetric water contents can be conveniently monitored with a calibrated neutron probe or a TDR system for the same depth increments.

As expected, the type of variables measured and their measurement locations, timing, and frequency can have a significant influence on the well-posedness and accuracy of the parameter estimation method. If the soil domain can be considered homogeneous, the unsaturated hydraulic parameters can be reasonably identified without much loss in parameter certainty by monitoring the change with time of matric head at a single depth and water content at two other depths close to the soil surface. It is most convenient to impose a constant total hydraulic head gradient (e.g., unit-gradient) at the lower boundary. The reduction in sampling depth, however, should not be at the expense of the measurement frequency. Data must be collected for the entire drainage experiment, especially since parameter sensitivities have shown to increase with drainage time. Generally, an accurate, simultaneous estimation of the hydraulic parameters requires between 6 and 10 measurement times during the drainage experiment.

For a hypothetical single-layer soil profile, 90 cm in depth, Santini and Romano (1992) discussed the parameter estimation procedure, using perturbed drainage

data to simulate random measurement errors. Successful results were obtained from measurements of a single tensiometer at the 30-cm depth in combination with water content values at depths of 30 and 60 cm. Other issues are discussed in the following comments:

1. The definition of the selected lower boundary condition of the draining soil requires careful consideration. To correctly select the appropriate boundary condition, accurate and numerous measurements of  $h_m$  at the lower boundary are needed during the course of the drainage experiment. Taking these measurements for proper definition of the lower boundary condition undoubtedly increases field operations and makes the experiment more time-consuming, but it is required for the accurate solution of Eq. [3.6.2–1]. In this regard, the assumption of a time-invariant hydraulic gradient at the bottom of the flow domain significantly reduces the number of measurements needed, and can be especially worthwhile if many field measurements are needed, such as in spatial variability studies (Romano, 1993). However, this assumption will require field verification. Alternatively, if appropriate, the  $\partial H/\partial z$  value at the lower boundary can be considered as an additional unknown constant parameter to be estimated by the inverse procedure together with the unsaturated soil hydraulic parameters.

2. Soil water content measurements should be taken frequently near the soil surface where their sensitivity to the hydraulic parameters is the greatest. The neutron probe is not recommended for near surface measurements, since its large measurement volume may extend to above the soil surface, especially under dry soil conditions. In contrast, TDR is especially suited for near surface measurements (Topp & Davis, 1985). Time domain reflectometry has the added advantage that it can provide automatic and real-time monitoring of soil water content (Baker & Allmaras, 1990). The depth location of the soil matric head sensors is less critical, as it has been shown that the sensitivity of the matric head to the hydraulic parameters is largely independent of soil depth in field drainage experiments.

3. The drainage method requires a large plot ( $\geq 12 \text{ m}^2$ ) to ensure that lateral water movement at the plot boundary will not influence the water regime in the plot center. In that regard, soil horizon characterization is important, since the presence of impeding horizons may induce lateral water movement and affect the required plot size. Moreover, an impeding layer can prevent unsaturated conditions below the impeding soil layer, thereby limiting the valid water content range of the optimized hydraulic parameters. Also, multilayered soil profiles can create perched water tables. Lateral water movement can be reduced by constructing an impermeable boundary around the plot perimeter to a depth slightly greater than the lower boundary of the soil domain.

### 3.6.2.6.c Simulation and Optimization

Equation [3.6.2–1] is solved for the following initial and boundary conditions

$$\begin{aligned} h_m(z) &= h_{m,i} & t = 0, 0 < z \leq L \\ q(z,t) &= 0 & t > 0, z = L \end{aligned} \quad [3.6.2-9]$$

where  $z = L$  denotes the soil surface, with  $L$  equal to the depth of the measured soil domain. Several types of boundary conditions can be considered at the bottom of the soil profile ( $z = 0$ ). Soil water content or pressure head values may be prescribed as a function of time, or a constant total hydraulic head gradient,  $\partial H/\partial z$ , can be used. Representing the lower boundary condition by a time-invariant unit hydraulic gradient can accurately describe observed drainage field studies (Libardi et al., 1980; Ahuja et al., 1988; McCord, 1991). Unknown hydraulic parameters are estimated by minimizing Eq. [3.6.2–5] using all  $h_m$  and  $\theta$  measurements. Additional comments include:

1. A limitation of the drainage experiment approach is that the experiment takes a long time (Baker et al., 1974) and that the experimental water content range is rather small. The presence of a shallow water table or slow drainage largely reduces the water content range. Even though the method can be extended to include surface evaporation, success of the inverse method is quite sensitive to the upper boundary condition and would therefore require accurate evaporation rate measurements.

2. Parameter optimization using drainage data can be especially useful for hydraulic characterization of field soils with little horizon differentiation, so that the average hydraulic behavior of the entire soil profile can be characterized. The inverse technique can be further exploited to provide effective soil hydraulic parameters for simulation of hydrological responses of large-scale areas (Kabat et al., 1997).

### 3.6.2.7 Additional Applications

Many more experimental techniques have demonstrated the potential benefits of inverse modeling to estimate soil hydraulic functions. Briefly, we summarize the upward infiltration method (Hudson et al., 1996), the sorptivity method (Section 3.5.3), the cone penetrometer method (Gribb, 1996), and the multistep extraction method (Inoue et al., 1998).

Both outflow and evaporation experiments represent water extraction processes and provide parameter estimates for the draining branches of the soil water content and hydraulic conductivity relationships. Parameters for the wetting branches of these soil hydraulic relationships are typically obtained from infiltration processes. The upward infiltration experiment suggested by Hudson et al. (1996) and the sorptivity method represent typical infiltration applications in the laboratory. For the upward infiltration experiment, packed cores are placed in a flow cell, similar to a Tempe cell (Section 3.3.2). However, the imposed flux boundary condition does not require the presence of a porous membrane at the bottom end of the flow cell. Instead, nylon fabric between the bottom end cap and the soil core allows for unrestricted water flux into the soil core. The top end plate of the cell includes a porous stainless-steel plate to prevent soil swelling, minimize surface evaporation, and allow escape of displaced air through the top of the cell. Moreover, tensiometers are placed horizontally at different vertical positions in the soil core. A TDR probe can be installed horizontally in the center of the soil core at the same vertical position as one of the tensiometers. However, Hudson et al. (1996) showed that little is gained by including water content measurements in the objective func-

tion. During the upward infiltration experiment, a constant water flux is imposed at the bottom of the soil sample and the matric head distribution within the soil sample is measured with one or more tensiometers. The latter should be installed only when the visible wetting front approaches each measurement location to prevent their malfunctioning at low initial matric head values. Upward infiltration rates can be controlled by a syringe pump to facilitate slow and constant movement of the one-dimensional wetting front through the soil core.

In the sorptivity method of Bruce and Klute (Klute & Dirksen, 1986), water is allowed to infiltrate under tension into a horizontal soil column. Using a Boltzmann transformation, the one-dimensional water content form of the flow equation can be solved analytically for this particular boundary condition, so that the soil water diffusivity can be computed as a function of water content. The analytical solution requires measurement of the soil water content distribution along the soil column for a specific time and supply head. In Šimůnek et al. (2000), the experimental results of Nielsen et al. (1962) are compared with the inverse solution for water supply heads of  $-2$ ,  $-50$ , and  $-100$  cm. Excellent agreement was found between the inverse solution and the analytical solution.

A modified cone penetrometer is instrumented with a porous filter close to the penetrometer tip and two tensiometer rings above the filter. The device is pushed into the soil to the desired depth, and a constant positive water head is applied to the filter for a short time period. While the volume of water imbibed by the soil is monitored, so is the response of both tensiometers to the advancing wetting front. Subsequently, after the water supply is cut off, the tensiometer measurements record the soil drying during water redistribution. The inverse method was used to estimate the hydraulic parameters of both the wetting and drying branches of the soil hydraulic characteristics by simultaneously analyzing the infiltration and redistribution data (Kodešová et al., 1999; Šimůnek et al., 1999a).

A multistep extraction device consists of a ceramic soil solution sampler inserted into a wetted soil and subjected to a series of vacuum extraction pressures. The cumulative amount of soil solution extracted, as well as the response of various tensiometers near the extractor are included in the objective function to estimate the soil hydraulic functions. The method was tested both in the laboratory and in the field (Inoue et al., 1998). The cone penetrometer and the extraction method require solution of a two-dimensional radial flow equation (Eq. [3.6.2–2]), and are typically applied in the field, potentially to large depths.

### 3.6.2.8 Example

We demonstrate the application of inverse modeling by comparing one-step and multistep outflow experiments for estimation of the hydraulic properties of a Columbia fine sandy loam (Wildenschild et al., 2001). We will illustrate the procedure in 12 consecutive steps. Practical comments are added where applicable to assist in solving the inverse problem. Although this example is specific to the outflow method, the same steps are required for all inverse methods.

**Step 1: Problem Definition.** This example determines the drainage curve of a Columbia fine sandy loam using inverse modeling. It is assumed that the underlying flow process is described by the Richards equation, (Eq. [3.6.2–1]), and that

the soil hydraulic properties are adequately represented by the coupled van Genuchten–Mualem model (Eq. [3.6.2–3] and [3.6.2–4]). Note that although these are common assumptions, they may not be appropriate in any specific case and may even cause unacceptable model errors.

The analysis was conducted for a disturbed soil sample that was packed to a predetermined bulk density after sieving the soil through a 0.5-mm sieve. Consequently, the hydraulic behavior is determined mostly by its texture. If the focus of the analysis were on the estimation of hydraulic properties near saturation, which are largely controlled by soil structure, an undisturbed soil sample should be used. In that case, however, the measurement of additional replicates, using larger soil cores, is recommended to account for the inherent field soil spatial variability. For the purpose of this example, inverse modeling results are compared with the classical one-step and multistep experiments.

**Step 2: Selection of Measurement Types.** As discussed in Section 3.6.2.3, outflow methods require a record of cumulative outflow as a function of time. Additionally, tensiometric data from the draining soil core will improve the well-posedness of the inverse solution. Although for this purpose measurements from a single tensiometer would be adequate, the presented example uses data from two tensiometers. The second tensiometer was included to allow simultaneous estimation of the unsaturated hydraulic conductivity. Moreover, the extra data may “save” the experiment if the other tensiometer fails.

**Step 3: Experimental Setup.** The basic requirements for outflow methods are described in Section 3.6.2.3. We selected the experimental setup of Wildenschild et al. (2001). A diagram of the flow cell (3.5 cm high and 7.62-cm i.d.) with gas and water flow controls is shown in Fig. 3.6.2–2. All connections consisted of quick-disconnect fittings (Cole-Parmer, Delrin, 1/4” NPT, 06359-72; Cole-Parmer Instrument Co., Vernon Hills, IL; [www.coleparmer.com](http://www.coleparmer.com)) so that the cell could be periodically detached for weighing to determine the water content at various times during drainage. Two tensiometers were inserted 1.1 cm (Tensiometer 1) and 2.4 cm (Tensiometer 2) from the top of the soil core, respectively. The tensiometer ports were offset laterally to minimize flow disturbance caused by the presence of the tensiometers. The tensiometers were made from 0.72-cm o.d., 0.1-MPa (1-bar), high-flow tensiometer cups (model 652X03-BIM3; Soilmoisture Corp., Santa Barbara, CA), glued to ~6-mm (1/4-inch) o.d. acrylic tubing. The tensiometers extended approximately 2 cm into the sample. Two 0.1-MPa (1-bar) transducers (model 136PC15G2 Honeywell, Minneapolis, MN) were used to monitor the matric head during the outflow experiments. Two additional ports were added on opposite sides of the cell to allow flushing the sample with CO<sub>2</sub> prior to wetting, so that complete saturation of the sample is ensured at the start of the experiment.

The outlet was connected to a burette for measurement of outflow as a function of time. The burette was mounted such that water drained at atmospheric pressure and was loosely covered with plastic to prevent evaporation. A 70-cm water pressure (1-psi) transducer (model 136PC01G2; Honeywell) was attached to the bottom of the burette to measure the cumulative drainage volume. The upper boundary condition was controlled using regulated pressurized N<sub>2</sub>. The N<sub>2</sub> was bubbled through a distilled water reservoir before entering the pressure cell to minimize evap-

oration losses from the soil core. Two layers of 1.2- $\mu\text{m}$ , 0.1-mm-thick nylon filters (MSI Masna nylon disc filters, Osmonic Laboratory Products; www.osmolab-store.com) were used as a porous membrane at the bottom of the sample. We combined two nylon filters to minimize puncturing, thereby ensuring a bubbling pressure of at least 700 cm during the outflow experiments. With a saturated hydraulic conductivity of approximately  $0.025 \text{ cm h}^{-1}$  (Table 3.6.2–1), the hydraulic resistance of the thin nylon membrane was low compared with other commonly used but thicker porous membranes with comparable bubbling pressure. Water pressure differences across our porous membrane are thus minimized during drainage of the soil core. All outflow experiments were conducted on the same soil core. The measured average saturated water content was  $0.445 \text{ cm}^3 \text{ cm}^{-3}$ . Time intervals for cumulative outflow and matric head measurements were approximately 10 s, which was sufficient to ensure that the rapid outflow after a gas pressure change was recorded with adequate temporal resolution.

**Step 4: Selection of Initial and Boundary Conditions.** The soil sample was initially fully saturated and then partially drained before the start of the outflow experiment so that the matric head at the bottom of the soil core ( $h_{\text{bottom}}$ ) was  $-2 \text{ cm}$ , corresponding with the following initial condition:

$$h_{m,i}(z) = -2 - z \quad t = 0, 0 < z < L \quad [3.6.2-10]$$

where  $z = L = 3.5 \text{ cm}$  is the height of the soil surface above a datum set at  $z = 0 =$  base of sample. Since the same sample was used for both the one-step and multi-step outflow experiments, the soil sample was resaturated prior to each drainage experiment, using the same procedure every time, including flushing with  $\text{CO}_2$  to ensure complete resaturation. This procedure ensured approximately identical initial saturation values between drainage experiments.

Full saturation at the onset of the experiment may be desired to provide reproducible initial conditions. However, for undisturbed soils, maximum saturation is usually  $<90\%$  of the total pore space. Therefore, it is recommended that hydraulic measurements of undisturbed field soils be conducted without  $\text{CO}_2$  flushing, so that the estimated soil hydraulic functions reflect the soil's natural behavior.

The boundary conditions of the one-step experiment are selected so that the air-entry value of the membrane is not exceeded. Moreover, applied pressure steps are soil specific and depend on soil texture. For our sandy loam soil, the pressure step applied was 500 cm, providing soil hydraulic data for a wide soil moisture range. Larger pressure steps may be required to drain a sufficient amount of water from a finer-textured soil. Accordingly, the boundary conditions for the one-step outflow experiment were

$$\begin{aligned} q(L,t) &= 0 \text{ cm d}^{-1} & t > 0 \\ h_m &= -500 \text{ cm} & 0 < t < t_e, z = 0 \text{ cm} \end{aligned} \quad [3.6.2-11]$$

where  $t_e$  denotes the duration of the one-step outflow experiment,  $q(0,t_e) \approx 0$ . The lower boundary condition was experimentally realized by increasing the applied  $\text{N}_2$

pressure at the top of the soil core to  $h_a = +500$  cm of water pressure, as expressed by Eq. [3.6.2–6].

For the multistep experiment, four pressure steps were applied in sequence, which covered the same pressure range as the one-step experiment. For each successive pressure step, time was allowed for the sample to equilibrate, as determined from a near zero drainage rate. The corresponding boundary conditions were

$$\begin{aligned}
 q(L,t) &= 0 \text{ cm d}^{-1} & t > 0 \\
 h_m &= -125 \text{ cm} & 0 > t > t_1, z = 0 \text{ cm} \\
 h_m &= -250 \text{ cm} & t_1 > t > t_2, z = 0 \text{ cm} \\
 h_m &= -375 \text{ cm} & t_2 > t > t_3, z = 0 \text{ cm} \\
 h_m &= -500 \text{ cm} & t_3 > t > t_4, z = 0 \text{ cm}
 \end{aligned} \tag{3.6.2–12}$$

**Step 5: Experimental Data.** The cumulative outflow ( $Q$ ) and matric head ( $h_m$ ) measurements are presented in Fig. 3.6.2–3a and 3.6.2–3b, for the one-step (O) and multistep (M) experiments, respectively. Although many more data points were collected than are shown in Fig. 3.6.2–3, we recommend not exceeding 100 data points per measurement type. The selected data must be representative of the whole set and include those measurements that describe the flow dynamics of the outflow experiment. Specifically, measurements prior to a pressure step increase must be included, and data should generally describe continuously increasing ( $Q$ ) or decreasing  $h_m$  values. Quality control of the raw data includes removal of spurious data caused by failure of the monitoring and data logging equipment, and comparison of  $h_m$  values with their expected equilibrium values at the end of each pressure step. Moreover, measurement uncertainty can be inferred from the time series of measurements.

**Step 6: Definition of the Objective Function.** The definition of the objective function is one of the most important steps in the inverse procedure. For the purpose of this example, we will compare optimizations with (+) and without (–) tensiometric data. As discussed in Section 3.6.2–2, selected weighting factors should be equal to the inverse of the expected measurement variances. However, in practice, this information may not be available. Moreover, for cases that include more than one measurement type, using measurement errors as weighting factors often resulted in local minima. It is, therefore, recommended to set all individual weighing factors ( $w_{i,j}$ ) in Eq. [3.6.2–5] equal to one and to compute weighing factors for the measurement types,  $v_j$ , that are reciprocal to their average magnitude multiplied with the number of data,  $n_j$ . For Measurement Type 1 (cumulative outflow), 2 (Tensiometer 1) and 3 (Tensiometer 2), the corresponding weights in Eq. [3.6.2–5] are then given by:

$$v_1 = 0.5/(n_1 \bar{Q}) \quad v_2 = 0.25/(n_2 \bar{h}_{m,1}) \quad v_3 = 0.25/(n_3 \bar{h}_{m,2})$$

where  $\bar{Q}$  denotes the time-averaged cumulative outflow value, and  $\bar{h}_{m,1}$  and  $\bar{h}_{m,2}$  represent the time-averaged tensiometric data of the top (Tensiometer 1) and bottom

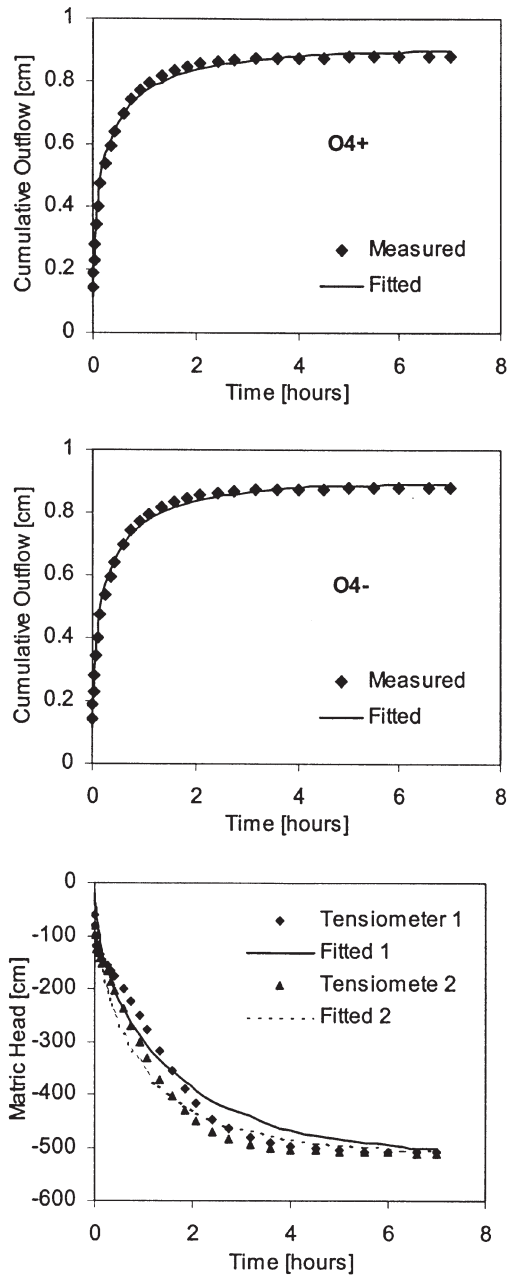


Fig. 3.6.2-3a. Measured (symbols) and optimized cumulative outflow and matric head curves for the one-step outflow experiment. In the notation of O4+ and O4-, the O stands for one-step outflow, the digit refers to the number of parameters to be optimized, and the + or - indicates the use or lack of use of tensiometric data, respectively. The 1 and 2 in the graph for the matric head data refer to the top and bottom tensiometer, respectively.

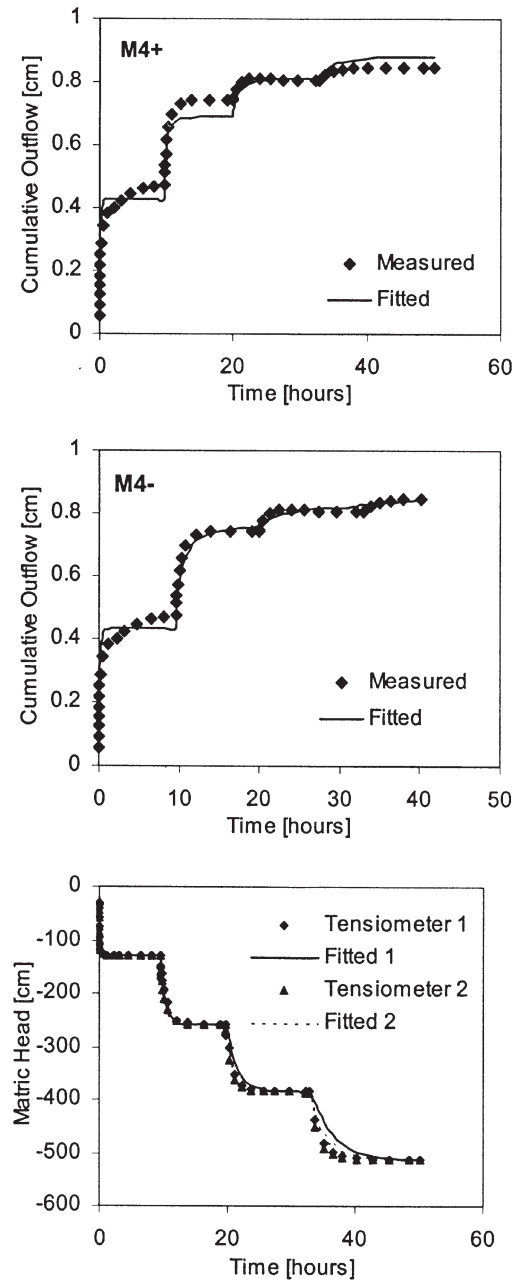


Fig. 3.6.2–3b. Measured (symbols) and optimized cumulative outflow and matric head curves for the multistep outflow experiment. In the notation of M4+ and M4–, the M stands for multistep outflow, the digit refers to the number of parameters to be optimized, and the + or – indicates the use or lack of use of tensiometric data, respectively. The 1 and 2 in the graph for the matric head data refer to the top and bottom tensiometer, respectively.

tensiometer (Tensiometer 2), respectively. In this example, the value of the objective function was calculated with  $v_j = 1/(n_j\sigma_j^2)$  and  $w_{i,j} = 1$ , where  $\sigma_j^2$  denotes the variance of all fitted data of measurement type  $j$  (Clausnitzer & Hopmans, 1995).

**Step 7: Selection of Fitting Parameters.** As stated in Section 3.6.1–3, the “classical” strategy in obtaining the van Genuchten–Mualem parameters is (i) to optimize  $\alpha$ ,  $n$ ,  $\theta_r$ , and  $K_s$  and to constrain the parameter  $m$  by the relation  $m = 1 - 1/n$ ; (ii) to determine  $\theta_s$  from an independent measurement; and (iii) to set the tortuosity parameter  $l$  to a fixed value of 0.5. However, since it has been increasingly demonstrated that improved fitting of the unsaturated hydraulic conductivity function is achieved with including  $l$  as a fitting parameter, we compare optimizations using  $l$  as a fitting parameter and as a fixed parameter set to 0.5 (Mualem, 1976). The saturated water content was fixed to its average value of  $0.455 \text{ cm}^3 \text{ cm}^{-3}$ .

**Step 8: Inverse Simulations.** Inverse simulations were conducted with the HYDRUS-1D code (Šimůnek et al., 1998b). Inverse simulation requires the same information as the forward problem, that is, time and geometric information, initial conditions, and boundary conditions, plus initial parameter estimates, position of observation points, and measurement times with corresponding data and weighing factors. Additionally, some convergence parameters need to be defined. It is, however, recommended to apply the default values as provided with HYDRUS-1D, which were determined from experience.

The soil sample was discretized using a variable grid spacing with 50 nodes, using finer spacings at the bottom of the soil column. The porous nylon membrane was not considered, since its resistance to water flow was negligible. If a ceramic porous plate is used, it must be explicitly represented in the model, as its hydraulic resistance will underestimate the soil’s hydraulic conductivity near saturation. The optimizations were repeated three times with different initial estimates for the parameters to be optimized. Conveniently, initial estimates were taken from the database that is included in HYDRUS-1D.

In total, we completed eight sets of inverse simulations (Table 3.6.2–2). The optimization results of the one-step (O) experiment will be compared with the multistep (M) experimental results for cases with tensiometric data (O4+, O5+, M4+, M5+) and without tensiometric data (O4–, O5–, M4–, M5–), using either four fitting parameters ( $l$  is fixed; cases denoted by 4) or five fitting parameters ( $l$  is an additional fitting parameter; cases denoted by 5).

For all multistep simulations, the inverse solution converged to similar optimization results, indicating that solutions were unique without local minima. This was different for the one-step simulations without tensiometric measurements (O4– and O5–), which converged towards various local minima depending on the initial parameter values. Although impractical, improved optimization results for these cases were obtained using initial parameter estimates equal to their optimized values of the one-step experiments with  $h_m$  measurements.

**Step 9. Comparison of Observed and Simulated Data. Residual Analysis.** After evaluation of the uniqueness of an inverse solution, the next logical step is to compare simulated results with the corresponding observations. Figures 3.6.2–3a and 3.6.2–3b show this comparison for the optimizations of the one-step (O4+ and

Table 3.6.2–2. Optimization results for one-step (O) and multistep (M) outflow experiments to estimate either four (O4+, O4–, M4+, and M4–) or five (O5+, O5–, M5+, and M5–) parameters with (+) or without (–) the help of tensiometric data. Values for the objective function and the average residuals were calculated according to Eq. [3.6.2–5] and [3.6.2–13], respectively. The values in parentheses in the last five columns refer to standard errors.

Case	Data	$\phi$	AR, $Q/h_m$	$R^2$	$\theta_r$	$\alpha$	$n$	$K_s$	$l$
			cm			cm <sup>-1</sup>		cm h <sup>-1</sup>	
O5+	$Q, h_m$	0.0112	0.0172/6.54	0.99	0.191 (0.00156)	0.00724 (0.00021)	4.05 (0.170)	0.126 (0.0081)	-1.23 (0.0167)
O4+	$Q, h_m$	0.0385	0.0135/23.7	0.99	0.0245 (0.0238)	0.0101 (0.00115)	1.57 (0.0787)	1.08 (0.288)	0.5 (fixed)
O5–	$Q$	0.00262	0.00917	0.99	0.0948 (0.0189)	0.00520 (0.00942)	2.29 (2.28)	0.219 (0.485)	-0.186 (1.05)
O4–	$Q$	0.00881	0.0123	0.99	0.0000 (0.00018)	0.00970 (0.00394)	1.52 (0.780)	1.08 (0.780)	0.5 (fixed)
M5+	$Q, h_m$	0.00960	0.0143/5.00	0.99	0.194 (0.00270)	0.00921 (0.00013)	3.02 (0.0110)	0.278 (0.0224)	-0.849 (0.0539)
M4+	$Q, h_m$	0.0249	0.0273/8.56	0.99	0.117 (0.01074)	0.0106 (0.00039)	1.86 (0.0755)	1.09 (0.09917)	0.5 (fixed)
M5–	$Q$	0.00625	0.0126	0.99	0.192 (0.00475)	0.00920 (0.00023)	3.06 (0.208)	0.358 (0.0488)	-0.318 (0.176)
M4–	$Q$	0.00835	0.0167	0.99	0.185 (0.00451)	0.00897 (0.00026)	3.11 (0.258)	0.534 (0.580)	0.5 (fixed)

O4–) and the multistep (M4+ and M4–) simulations, respectively. The respective optimization results are presented in Table 3.6.2–2. The comparison shows that the general dynamics of the measurements is matched by all simulations. This is a necessary, but not sufficient condition to evaluate the accuracy of the optimized hydraulic parameters. Upon closer inspection, we notice the presence of small systematic deviations between measured and predicted values, indicating that errors are autocorrelated. Moreover, it is apparent that not all four models fit the measured data equally well.

Regarding the systematic deviations, outflow data for the multistep experiment show that during the first pressure step the simulated outflow reaches equilibrium much faster than the observed data (Fig. 3.6.2–3b). This is not uncommon and indicates that the process model (Richards' equation) is unable to accurately describe the true flow behavior in the near-saturated water content region. This effect is most likely caused by the presence of a discontinuous air phase at matric head values near the soil's air-entry value (Schultze et al., 1999; Wildenschild et al., 2001). Improved fitting of the measured data can be achieved by either applying the first pressure step after the soil is first slightly desaturated or by solving the multiphase flow problem. Other deviations of the simulated multistep outflow curves can be related to the assumption of a fixed  $l$  parameter in the unsaturated conductivity model (Durner et al., 1999b).

When comparing cumulative outflow ( $Q$ ) residuals (Column 4 in Table 3.6.2–2) between the one-step and the multistep method, it appears that the one-step method gives better results (i.e., the fit is better). However, it must be intuitively clear that as the number and complexity of different measurement types increase, the difficulty of fitting all combined data will increase as well, especially if the op-

timization problem contains model and/or measurement errors. Because of this, case O5– (one-step method without tensiometric measurements and five fitting parameters) produces the lowest  $\phi$  value of all eight cases (Table 3.6.2–2, third row). Inspection of Table 3.6.2–2 also clearly shows that the fitting of the cumulative outflow data is much improved if the connectivity parameter,  $l$ , in the conductivity expression is allowed to vary: the  $\phi$  values for the five-parameter cases ( $l$  fitted) are always much lower than for the four-parameter cases, where  $l$  is fixed at 0.5.

The average residual (Column 4 in Table 3.6.2–2) includes the average deviation between the measured and fitted  $Q$  or  $h_m$  values. These values can be compared with the measurement error of each measurement type for model adequacy testing. Conservative estimates of measurement errors for the tensiometer and burette measurements are 1 and 0.011 cm, respectively. The burette measurement error corresponds with 0.5 mL of drainage for a soil core radius of 3.81 cm (sample area of 45.6 cm<sup>2</sup>). By inspection of Table 3.6.2–2, it is clear that the time-averaged residual (AR) of the matric head (measurement type  $j = 2$  and 3), defined as:

$$\text{AR}(h_m) = \sum_{j=2}^3 (1/n_j) \sum_{i=1}^{n_j} [h_{m,j-1}^*(t_i) - h_{m,j-1}(t_i, \boldsymbol{\beta})]^2 \quad [3.6.2-13]$$

is larger than the conservative measurement error in all cases (for notation, see Eq. [3.6.2–5]). Specifically, the lowest average residual is 5 cm (case M5+, Table 3.6.2–2), whereas the assumed measurement error was only 1 cm. When considering the average residual for cumulative outflow (measurement type  $j = 1$  only; replace  $h_m$  by  $Q$  in Eq. [3.6.2–13]), the AR of almost all cases is about equal to or slightly larger than the assumed measurement error of 0.011 cm. This is specifically so for the one-step experiments without  $h_m$  measurements (cases O4– and O5–), since these are the easiest to fit.

These considerations, in addition to the observations of the residual analysis, which showed that the deviations between measurements and observations are not randomly distributed, allow us to assess the adequacy of the flow model. We conclude that the combined measurement and model error for the outflow experiment using the described experimental conditions is larger than the precision of the measurement devices. The larger errors are caused by assuming that (i) the Richards' type water flow equation, in combination with its numerical solution and the selected hydraulic model, is the correct physical model for simulating drainage of the one-step and multistep experiments and/or (ii) the experimental conditions are such that they exactly conform to the assumptions of the flow model. Clearly, the divergence between observed and measured outflow during the first two steps of the multistep method indicate that these assumptions are not fully met (Fig. 3.6.2–3b). For example, although analytical models have proven useful in integrating knowledge of soil hydraulic properties for numerical models and other applications, they rarely fit the measured retention data exactly, thereby introducing AR values larger than the measurement error. For a more thorough discussion of the influence of model errors on the interpretation of inverse modeling results see Durner et al. (1999a, b).

*Correlation of Simulated and Observed Data.* The fifth column of Table 3.6.2–2 lists the  $R^2$  values that quantify the correlation between measured and sim-

ulated flow variables (for an optimum parameter set  $\beta$ ). As all correlation values are very high, their magnitude is of little value for model adequacy testing.

Summarizing the results, we conclude that the residual errors are small enough to accept the assumed flow and hydraulic models for soil hydrological applications. Accordingly, we proceed further.

**Step 10: Analysis of Parameter Values and Hydraulic Functions.** *Parameter Uncertainty.* Columns 6 through 10 of Table 3.6.2–2 list the optimized hydraulic parameters. The values in parentheses denote the standard error of estimation as determined from the 95% confidence intervals around the optimized value. The standard errors of all fitted parameters are computed from  $(C_{ii})^{1/2}$ , where  $C_{ii}$  is the diagonal element of the parameter covariance matrix  $\mathbf{C}$  (see Section 1.7, Eq. [1.7–23]). It was already concluded from the residual analysis that these standard error values are not very useful statistically, since the requirement of independent residuals is violated. However, their relative magnitude may be useful when comparing parameters and hydraulic models.

*Parameter Correlation.* Table 3.6.2–3 shows correlation coefficients between the optimized parameters for all eight cases. Values larger than  $\pm 0.90$  are bolded. Obviously, high correlation between parameters unnecessarily increases the number of optimized parameters. High correlation causes underestimation of parameter uncertainty, slows down convergence rate, and increases nonuniqueness. It is expected that the number of highly correlated parameters increases as the number of fitted parameters increases. As a result, the available information in the objective function is reduced. Table 3.6.2–3 confirms that the highest number of correlations occur for cases O4– and O5–, that is, the one-step outflow experiment without matrix head measurements. As discussed in Section 3.6.2–3, the information content of these experiments is not sufficient to obtain unique parameters. The data show large correlations between  $n$  and  $\theta_r$  for the multistep experiments, a result that is common when fitting retention data to the van Genuchten relationship if information for the dry range is missing.

*Hydraulic Functions.* The optimized soil water retention and unsaturated hydraulic conductivity functions for all four cases using four fitting parameters are presented in Fig. 3.6.2–4. The optimized functions are accurate only for the experimental water content range of the outflow experiment (i.e.,  $h_m > -500$  cm), and care must be exercised in their extrapolation to drier soil conditions.

Independent soil water retention data (thick solid line) were obtained by a syringe pump procedure (Wildenschild et al., 1997) in a separate experiment by which the soil sample was drained at a constant, low flow rate of  $0.5 \text{ mL h}^{-1}$ , simulating quasistatic conditions at any time during the drainage experiment. The conditions of the steady-state experiment are considered optimal; therefore, the optimized retention curves are compared with the retention data from the syringe experiment using cumulative drainage with corresponding tensiometric data. Unfortunately, it was impossible to estimate the hydraulic conductivity from the syringe pump experiments because of errors resulting from the extremely small hydraulic head gradients. Consequently, the optimized curves are compared with independently estimated unsaturated hydraulic conductivity data reported in Wildenschild et al. (2001).

Table 3.6.2-3. Correlation matrices for the van Genuchten parameters for one-step (O) and multistep (M) outflow experiments to estimate either four (O4+, O4-, M4+, and M4-) or five (O5+, O5-, M5+, and M5-) parameters with (+) or without (-) the help of tensiometric data.

Parameter	Case	$\theta_r$	$\alpha$	$n$	$K_s$	$l$
$\theta_r$	O5+	1				
	O4+					
	O5-					
	O4-					
$\alpha$	O5+	-0.162	1			
	O4+	-0.363				
	O5-	-0.282				
	O4-	-0.683				
$n$	O5+	0.581	-0.761	1		
	O4+	0.864	-0.774			
	O5-	0.346	<b>-0.998</b>			
	O4-	-0.662	<b>-0.999</b>			
$K_s$	O5+	-0.104	0.673	0.715	1	
	O4+	-0.352	<b>0.992</b>	-0.765		
	O5-	-0.323	<b>0.998</b>	<b>-0.998</b>		
	O4-	-0.661	<b>0.998</b>	<b>-0.992</b>		
$l$	O5+	0.083	0.037	-0.063	0.715	1
	O4+	--	--	--	--	
	O5-	0.161	<b>0.981</b>	<b>0.971</b>	<b>-0.966</b>	
	O4-	--	--	--	--	
$\theta_r$	M5+	1				
	M4+					
	M5-					
	M4-					
$\alpha$	M5+	-0.499	1			
	M4+	-0.481				
	M5-	-0.547				
	M4-	-0.650				
$n$	M5+	<b>0.913</b>	-0.737	1		
	M4+	<b>0.950</b>	-0.715			
	M5-	0.887	-0.804			
	M4-	<b>0.912</b>	-0.840			
$K_s$	M5+	-0.368	0.255	-0.408	1	
	M4+	-0.267	0.621	-0.412		
	M5-	-0.347	-0.056	-0.080		
	M4-	-0.006	0.158	-0.170		
$l$	M5+	-0.330	0.111	0.322	0.811	1
	M4+	--	--	--	--	
	M5-	-0.235	-0.172	0.077	0.751	
	M4-	--	--	--	--	

When comparing the functions, the results are surprisingly close. Note, however, that the optimization results of the one-step experiment without tensiometric measurements (O4-) were obtained by using initial, optimized values from the optimization with  $h_m$  measurements (O4+) as initial parameter values. We also find that the tensiometric measurements in the multistep experiments gave results similar to multistep experiments without tensiometric data, especially for cases with an optimized  $l$ . This may be caused partly by our experimental strategy to wait for static equilibrium before increasing the applied gas pressure. Generally speaking, it shows that for the conditions of our experiment, the use of outflow data alone from a multistep experiment may be sufficient to obtain the correct hydraulic properties

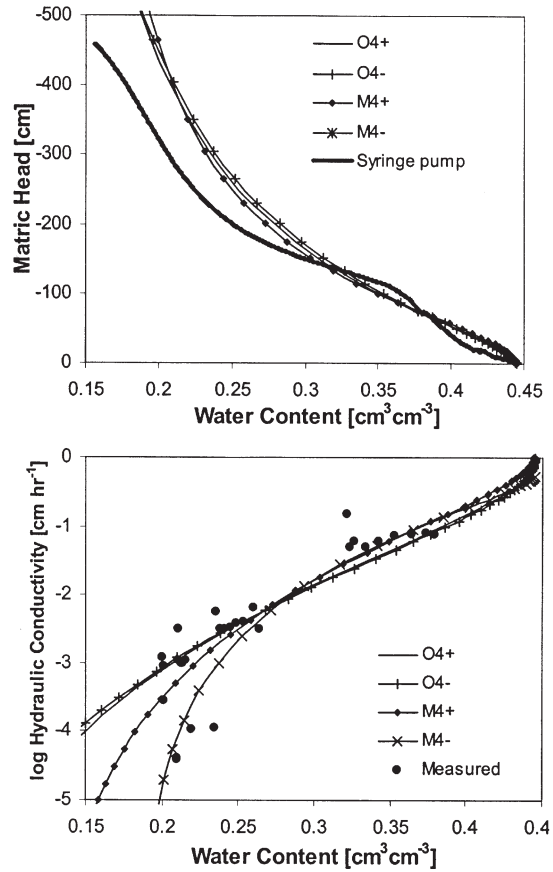


Fig. 3.6.2-4. Comparison of optimized and independently measured retention and unsaturated hydraulic conductivity data for the four parameter optimizations ( $l = 0.5$ ). For an explanation of the notation of O4+, O4-, M4+, and M4-, see the figure captions of Fig. 3.6.2-3a,b.

by inverse simulation. The unsaturated hydraulic conductivity comparison in Fig. 3.6.2-4 also supports the general conclusion that multistep experiments are preferred over one-step experiments.

**Step 11: Response Surface Analysis.** The evaluation of response surfaces is usually done a priori to design the experimental conditions for inverse modeling using forward simulations. We like to illustrate these analysis in this final step to support the concepts introduced in Section 3.6.2-2.

*Response Surface Analysis.* Response surface analysis can be used to investigate the posedness of the optimization problem. The behavior of the objective function within a multiparameter space can only be visualized by limiting the number of variable parameters to two. Consequently, the value of the objective function,  $\phi$ , can be shown for combinations of two parameters, while keeping all other parameters at their “true” (i.e., optimized) values. It thus follows that response surfaces

can only be calculated posteriori if the true optimum is known as determined from forward modeling results.

The case with four adjustable parameters requires analysis of six possible parameter pairs. Figure 3.6.2–5a shows response surfaces for  $(n, \alpha)$ ,  $(K_s, \alpha)$ ,  $(\theta_r, \alpha)$ ,  $(\theta_r, K_s)$ ,  $(K_s, n)$ , and  $(\theta_r, n)$  for the one-step experiment without  $h_m$  measurements (case O4– in Table 3.6.2–3). Along a response surface, the optimum two-parameter combination is determined by a  $\phi$  valley or minimum enclosed by contour lines. The shape of the valley indicates the rate of convergence, degree of parameter correlation, parameter sensitivity, and presence of local minima. When comparing response surfaces, the parameter sensitivity decreases as the  $\phi$  interval increases. The ideal response surface shows a narrow minimum area with circular shape, indicating no correlation between fitting parameters. Response surfaces that are parallel to one of the axes are insensitive to that respective parameter, indicating high parameter uncertainty and a large confidence interval. Unfavorable response surfaces consist of long narrow valleys with an approximate angle of  $45^\circ$ , indicating a high correlation between parameters, while L-shaped valleys indicate slow convergence.

The response surfaces calculated from real data, contrary to those obtained from numerically generated data, are much more difficult to interpret since the residuals are not necessarily normally distributed and may exhibit some systematic bias. The response surfaces of the ill-posed one-step experiment in Fig. 3.6.2–5a are unfavorable because of (i) multiple minima within a low  $\phi$  value valley (response surface  $\theta_r, n$ ), (ii) extremely narrow valleys for parameter combinations  $\theta_r, n$  and  $K_s, n$ , and (iii) wide interval spacings. When comparing the results of Fig. 3.6.2–5a with those of Fig. 3.6.2–5b (multistep with  $h_m$  data), we note that interval spacings are smaller and that most minima are elliptical in shape. Still, the  $K_s$  parameter appears to be the least sensitive, which is not surprising when considering that almost all data in the objective function are related to unsaturated flow.

Response surfaces are usually calculated to describe the behavior of the objective function in the cross sections of the two-parameter plane for the multiparameter space. However, they cannot illustrate the shape of the objective function in other parts of the parameter space. Thus, if response surfaces do not display well-defined minima, the parameter optimization problem is certainly ill-posed (Figure 3.6.2–5a, parameter pair  $\theta_r, n$ ). There is, however, no guarantee that the problem is well-posed if well-defined minima are demonstrated for all parameter pairs. This is because minimization (especially for gradient-type methods; see Section 1.7) can lead to optimized parameters for any local minimum of the objective function, far away from the global minimum. For example, although the response surfaces for the one-step and multistep experiments look fairly similar (Fig. 3.6.2–5a and 3.6.2–5b), the response surfaces for the one-step method were obtained after using initial parameter estimates that were close to the actual global minimum. Thus, response surface analyses can show that a specific experimental setup will result in an ill-posed optimization problem, but it cannot guarantee a well-posed optimization problem by itself.

**Summary and Conclusions.** Analysis of the one-step data without considering tensiometric information suffered from large uncertainties and cross corre-

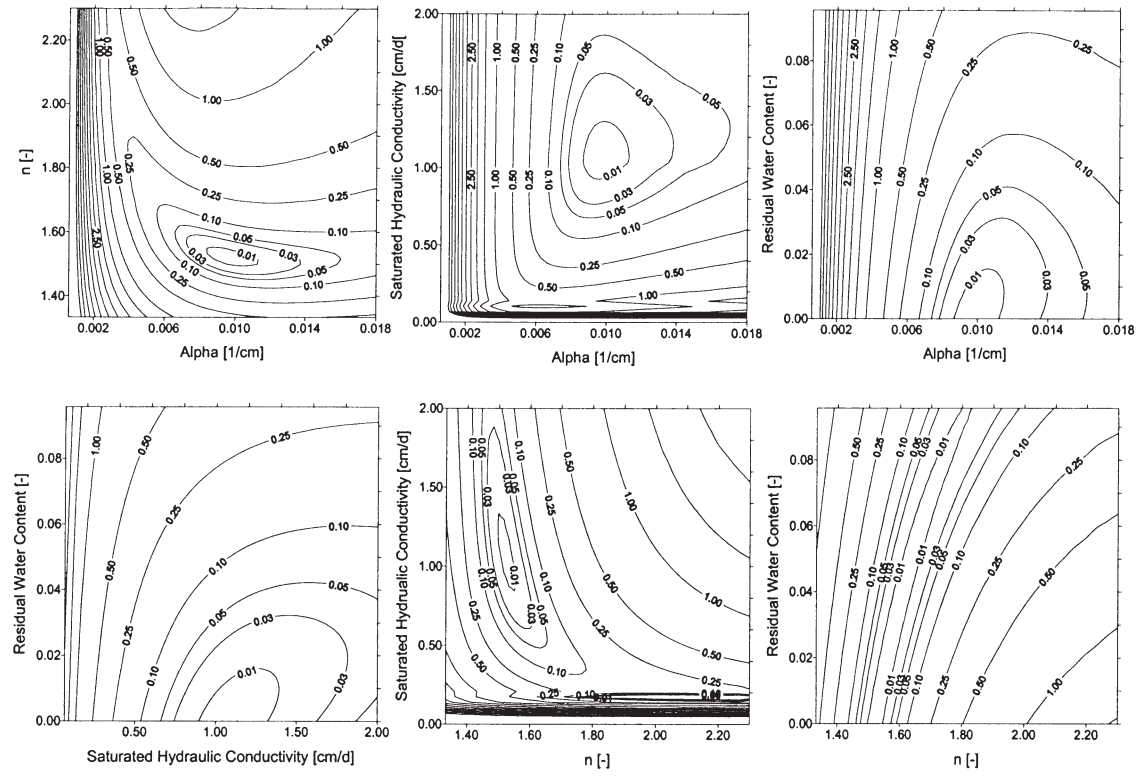


Fig. 3.6.2-5a. Response surfaces for the one-step experiment without tensiometric data (O4-).

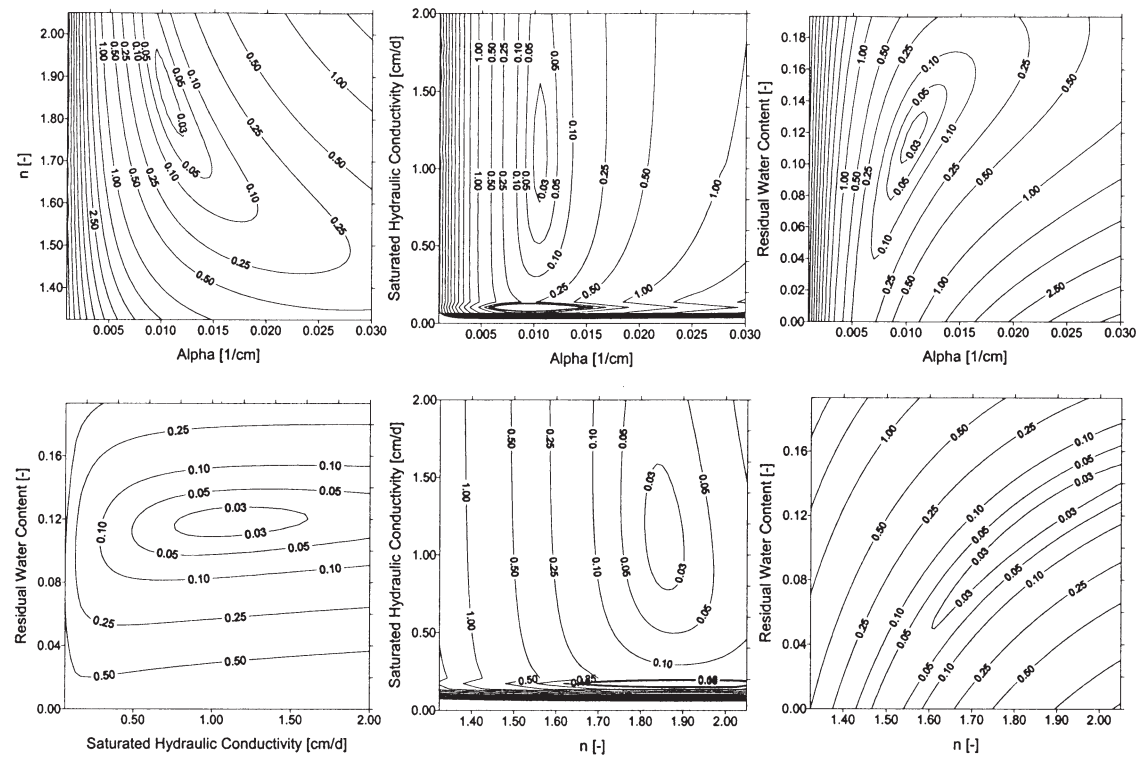


Fig. 3.6.2-5b. Response surfaces for the multistep experiment with tensiometric data (M4+).

lation among parameters, with optimized parameters strongly dependent on their initial estimates. Results for the multistep experiment (both with and without additional tensiometric information) and the one-step experiment with measured matric head values were fairly similar. This was especially the case when the  $l$  parameter was allowed to be optimized as well. However, significant smaller confidence intervals were obtained when combining matric head and cumulative outflow data in the objective function. Thus, although matric head data are not required for inverse modeling of a multistep outflow experiment, their inclusion may lead to smaller confidence intervals of the optimized parameters. Tensiometric data are required when conducting a one-step outflow experiment to avoid nonuniqueness problems. Finally, the analysis has shown that the inverse modeling of multistep outflow can provide accurate and reliable estimates of both the retention and the unsaturated hydraulic conductivity curve parameters for the intermediate soil water content range.

### 3.6.2.9 Discussion

Soil hydraulic parameter estimation by inverse modeling is a relatively complex procedure that provides a quick method for soil hydraulic characterization, yielding parameters for both the soil water retention and unsaturated hydraulic conductivity function from a single experiment. Its successful application requires suitable experimental procedures as well as advanced numerical flow codes and optimization algorithms. Numerical codes with user-friendly interfaces are becoming available that can be used for both inverse and direct simulations (e.g., Šimůnek et al., 1998b, 1999b). However, since the method as a whole is not fully developed yet, both experimental and numerical modeling expertise is required for successful application of the methodology and correct interpretation of the results.

When compared with other measurement methods, the inverse modeling approach renders a suite of benefits. First and foremost, it mandates the combination of experimentation with numerical modeling. Since the optimized hydraulic functions are mostly needed as input to numerical flow and transport models for prediction purposes, it is an added advantage that the hydraulic parameters are estimated using similar numerical models as used for predictive forward modeling. An additional benefit of the inverse procedure is their application to transient experiments, thereby providing relatively fast results. Finally, the parameter optimization procedure computes confidence intervals of the optimized parameters, although their interpretation can be misleading.

Inverse problems for parameter estimation of soil hydraulic functions can be ill-posed because of inadequate experimental design, measurement errors, and model errors. Analysis of such flow problems must include a search for the optimum number of flow variables required in the objective function. For example, as the number of optimized parameters increases, increased information content of the measurements is required, for example, by including observations of different types, or by using time-variable boundary conditions. Sensitivity analysis can largely optimize the need for type, number, and spatial location of the measurements. For example, it has been shown in a variety of applications that measured transient flow data, as induced by multiple step changes at the domain boundary, are more sensitive to the estimated parameters than using a single step. Also, an increase in

the number of parameters to be optimized will generally lead to a reduction in model error, but will increase the parameter uncertainty. A well-posed problem requires a priori testing for nonuniqueness using response surface analysis and parameter sensitivity and correlation. Insensitive parameters should be measured independently, whereas highly correlated parameters will affect uniqueness of the inverse problem, requiring independent measurement of one of the correlated parameters. To reduce nonuniqueness and to extend the range of application beyond the experimental range of measurements, independently measured information on the soil hydraulic functions can be included in the objective function. This prior information can reduce parameter uncertainty, but may reduce the goodness of fit between model and data.

As with all other laboratory and field methods to estimate soil hydraulic functions, it is assumed that the functional forms used are capable of accurately describing the soil hydraulic data. It is therefore essential to perform a model adequacy test by comparing objective function residuals with measurement errors, to identify model errors. Obviously, if the parametric models (Section 3.3.4) are not adequate for a tested soil, the resulting fitting parameters will not be valid. Especially, if the coupled Mualem approach is used, their improper selection may compromise the accuracy of both hydraulic functions.

When comparing the optimized hydraulic functions with the results of other methods, one must consider differences in model assumptions and experimental range. Laboratory measurements, although accurate, provide hydraulic information for a relatively small soil core, detached from its surroundings. On the other hand, field experiments will generally include the continuum of soil horizons that will influence water flow and the estimated soil hydraulic functions. Moreover, as is the case for any method, the parameter estimates are only valid for the range of the experimental conditions, and care must be exercised in their extrapolation.

This chapter must be regarded as a work in progress, since the mathematical, analytical, and experimental procedures that constitute the inverse method as a whole are still an area of intensive research. Improvements in parameter estimation methods in combination with experimental requirements and optimization algorithms continue to appear in a steady stream of publications. Nevertheless, the general inverse method has demonstrated to be an excellent new tool that allows for soil hydraulic characterization using a wide spectrum of transient laboratory and field experiments. To date, the application of the inverse parameter estimation method in the vadose zone has been limited to the estimation of soil hydraulic properties. This is not surprising because hydraulic parameters are required in most flow and transport models and their direct measurements are time-consuming. We pose that inverse modeling can be used to estimate other soil properties as well, such as solute transport, heat flow, and gaseous transport parameters. Moreover, the methodology can be applied to better understand processes, such as differentiation between matrix and macropore contributions to water flow for two-domain simulation models (Šimnek et al., 2001), or to infer root water uptake parameters in crop growth simulation models (Vrugt et al., 2001a). Summarizing, we conclude that parameter estimation by inverse modeling has tremendous potential in characterizing vadose flow and transport processes, while simultaneously presenting us with an additional tool to better understand their fundamental mechanisms.

### 3.6.2.10 References

- Ahuja, L.R., B.B. Barnes, D.K. Cassel, R.R. Bruce, and D.L. Nofziger. 1988. Effect of assumed unit gradient during drainage on the determination of unsaturated hydraulic conductivity and infiltration parameters. *Soil Sci.* 145:235–243.
- Ankeny, M.D., M. Ahmed, T.C. Kaspar, and R. Horton. 1991. Simple field method for determining unsaturated hydraulic conductivity. *Soil Sci. Soc. Am. J.* 55:467–470.
- Baker, F.G., P.L.M. Veneman, and J. Bouma. 1974. Limitations of the instantaneous profile method for field measurement of unsaturated hydraulic conductivity. *Soil Sci. Soc. Am. J.* 38:885–888.
- Baker, J.M., and R.R. Allmaras. 1990. System for automating and multiplexing soil moisture measurement by time-domain reflectometry. *Soil Sci. Soc. Am. J.* 54:1–6.
- Bear, J. 1972. *Dynamics of fluids in porous media*. American Elsevier, New York, NY.
- Becher, H.H. 1971. Ein Verfahren zur Messung der ungesättigten Wasserleitfähigkeit. *Z. Pflanzenernaehr. Bodenkd.* 128:1–12.
- Boels, D., J.B.H.M. van Gils, G.J. Veerman, and K.E. Wit. 1978. Theory and system of automatic determination of soil moisture characteristics and unsaturated hydraulic conductivities. *Soil Sci.* 126:191–199.
- Brooks, R.H., and A.T. Corey. 1966. Properties of porous media affecting fluid flow. *J. Irrig. Drain. Div. Am. Soc. Civ. Eng.* 92:61–88.
- Celia, M.A., E.T. Bouloutas, and R.L. Zarba. 1990. A general mass-conservative numerical solution for the unsaturated flow equation. *Water Resour. Res.* 26:1483–1496.
- Chen, J., J.W. Hopmans, and M.E. Grismer. 1999. Parameter estimation of two-fluid capillary pressure-saturation and permeability functions. *Adv. Water Resour.* 22:479–493.
- Ciollaro, G., and N. Romano. 1995. Spatial variability of the soil hydraulic properties of a volcanic soil. *Geoderma* 65:263–282.
- Clausnitzer, V., and J.W. Hopmans. 1995. Nonlinear Parameter estimation. LM-OPT. General purpose optimization code based on the Levenberg–Marquardt algorithm. LAWR Report 100032. University of California, Davis, CA.
- Cuenca, R.H., J. Brouwer, A. Chanzy, P. Droogers, S. Galle, S.R. Gaze, M. Sicot, M., H. Stricker, R. Angulo-Jaramillo, S.A. Boyle, J. Bromly, A.G. Chebhouni, J.D. Cooper, A.J. Dixon, J.-C. Fies, M. Gandah, J.-C. Gaudu, L. Laguerre, M. Soet, H.J. Steward, J.-P. Vandervaere, and M. Vauclin. 1997. Soil measurements during HAPEX-Sahel intensive observation period. *J. Hydrol.* 188–189:224–266.
- Dane, J.H., and S. Hruska. 1983. In-situ determination of soil hydraulic properties during drainage. *Soil Sci. Soc. Am. J.* 47:619–624.
- Dirksen, C. 1991. Unsaturated hydraulic conductivity, p. 209–269. *In* K.A. Smith and C.E. Mullins (ed.) *Soil analysis: Physical methods*. Marcel Dekker, New York, NY.
- Doering, E.J. 1965. Soil water diffusivity by the one-step method. *Soil Sci.* 99:322–326.
- Durner, W. 1994. Hydraulic conductivity estimation for soils with heterogeneous pore structure. *Water Resour. Res.* 30:211–233.
- Durner, W., E. Priesack, H.-J. Vogel, and T. Zurmühl. 1999a. Determination of parameters for flexible hydraulic functions for inverse modeling, p. 817–827. *In* M.Th. van Genuchten et al. (ed.) *Characterization and measurement of the hydraulic properties of unsaturated porous media*. University of California, Riverside, CA.
- Durner, W., E.B. Schultze and T. Zurmühl. 1999b. State-of-the-art in inverse modeling of inflow/outflow experiments, p. 661–681. *In* M.Th. van Genuchten et al. (ed.) *Characterization and measurement of the hydraulic properties of unsaturated porous media*. University of California, Riverside, CA.
- Eching, S.O., and J.W. Hopmans. 1993a. Optimization of hydraulic functions from transient outflow and soil water pressure data. *Soil Sci. Soc. Am. J.* 57:1167–1175.
- Eching, S.O., and J.W. Hopmans. 1993b. Inverse solution of unsaturated soil hydraulic functions from transient outflow and soil water pressure data. Land, Air and Water Resources Paper No. 100021. Univ. of California, Davis, CA.
- Eching, S.O., J.W. Hopmans, and O. Wendroth. 1994. Unsaturated hydraulic conductivity from transient multi-step outflow and soil water pressure data. *Soil Sci. Soc. Am. J.* 58:687–695.
- Feddes, R.A., P. Kabat, P.J.T. van Bakel, J.J. B. Bronswijk, and J. Habertsma. 1988. Modeling soil water dynamics in the unsaturated zone—State of the art. *J. Hydrol.* 100:69–111.
- Gardner, W.R. 1956. Calculation of capillary conductivity from pressure plate outflow data. *Soil Sci. Soc. Am. Proc.* 20:317–320.
- Gardner, W.R. 1958. Some steady-state solutions of the unsaturated moisture flow equation with application to evaporation from a water table. *Soil Sci.* 85:228–232.

- Gardner, W.R. 1962. Note on the separation and solution of diffusion type equations. *Soil Sci. Soc. Am. Proc.* 26:404.
- Gardner, W.R., and F.J. Miklich. 1962. Unsaturated conductivity and diffusivity measurements by a constant flux method. *Soil Sci.* 93:271–274.
- Gribb, M.M. 1996. Parameter estimation for determining hydraulic properties of a fine sand from transient flow measurement. *Water Resour. Res.* 32:1965–1974.
- Gupta, S.C., D.A. Farrell, and W.E. Larson. 1974. Determining effective soil water diffusivities from one-step outflow experiments. *Soil Sci. Soc. Am. Proc.* 38:710–716.
- Halbertsma, J.M., and G.J. Veerman. 1994. A new calculation procedure and simple set-up for the evaporation method to determine soil hydraulic functions. Report 88. DLO Winand Staring Centre, Wageningen, The Netherlands.
- Hillel, D., V.D. Krentos, and Y. Stylianou. 1972. Procedure and test of an internal drainage method for measuring soil hydraulic characteristics in situ. *Soil Sci.* 114:395–400.
- Hollenbeck, K.J., and K.H. Jensen. 1998a. Maximum-likelihood estimation of unsaturated hydraulic parameters. *J. Hydrol.* 210:192–205.
- Hollenbeck, K.J., and K.H. Jensen. 1998b. Experimental evidence of randomness and nonuniqueness in unsaturated outflow experiments designed for hydraulic parameter estimation. *Water Resour. Res.* 34:595–602.
- Hollenbeck, K.J., J. Šimnek, and M.Th. van Genuchten. 2000. RETCML: Incorporating maximum-likelihood estimation principles in the soil hydraulic parameter estimation code RETC. *Comput. Geosci.* 26:319–327.
- Hopmans, J.W., and J. Šimnek. 1999. Review of inverse estimation of soil hydraulic properties. p. 643–659. *In* M.Th. van Genuchten et al. (ed.) *Characterization and measurement of the hydraulic properties of unsaturated porous media*. University of California, Riverside, CA.
- Hopmans, J.W., T. Vogel, and P.D. Koblik. 1992. X-ray tomography of soil water distribution in one-step outflow experiments. *Soil Sci. Soc. Am. J.* 56:355–362.
- Hudson, D.B., P.J. Wierenga, and R.G. Hills. 1996. Unsaturated hydraulic properties from upward flow into soils cores. *Soil Sci. Soc. Am. J.* 60:388–396.
- Inoue, M., J. Šimnek, J.W. Hopmans, and V. Clausnitzer. 1998. In situ estimation of soil hydraulic functions using a multi-step extraction technique. *Water Resour. Res.* 34:1035–1050.
- Kabat, P., R.W.A. Hutjes, and R.A. Feddes. 1997. The scaling characteristics of soil parameters: From plot scale heterogeneity to subgrid parameterization. *J. Hydrol.* 190:363–396.
- Klute, A., and C. Dirksen. 1986. Conductivities and diffusivities of unsaturated soils. p. 687–734. *In* A. Klute (ed.) *Methods of soil analysis*. Part 1. 2nd ed. Agron. Monogr. 9. ASA and SSSA, Madison, WI.
- Kodešová, R., S.E. Ordway, M.M. Gribb, and J. Šimnek. 1999. Estimation of soil hydraulic properties with the cone permeameter: Field studies. *Soil Sci.* 164:527–541.
- Kool, J.B., and J.C. Parker. 1988. Analysis of the inverse problem for transient unsaturated flow. *Water Resour. Res.* 24:817–830.
- Kool, J.B., J.C. Parker, and M.Th. van Genuchten. 1987. Parameter estimation for unsaturated flow and transport models—A review. *J. Hydrol.* 91:255–293.
- Kool, J.B., J.C. Parker, and M.Th. van Genuchten. 1985. Determining soil hydraulic properties for one-step outflow experiments by parameter estimation. I. Theory and numerical studies. *Soil Sci. Soc. Am. J.* 49:1348–1354.
- Kulkarni, R., A.T. Watson, J.E. Nordtvedt, and A. Sylte. 1998. Two-phase flow in porous media: Property identification and model validation. *AICHE J.* 44:2337–2350.
- Libardi, P.L., K. Reichardt, D.R. Nielsen, and J.W. Biggar. 1980. Simple field methods for estimating soil hydraulic conductivity. *Soil Sci. Soc. Am. J.* 44:3–7.
- Liu, Y.P., J.W. Hopmans, M.E. Grismer, and J.Y. Chen. 1998. Direct estimation of air–oil and oil–water capillary pressure and permeability relations from multi-step outflow experiments. *J. Contam. Hydrol.* 32:223–245.
- Logsdon, S.D., E.L. McCoy, R.R. Allmaras, and D.R. Linden. 1993. Macropore characterization by indirect methods. *Soil Sci.* 155:316–324.
- McCord, J.T. 1991. Application of second-type boundaries in unsaturated flow modeling. *Water Resour. Res.* 27:3257–3260.
- Mortensen, A.P., R.J. Glass, and K. Hollenbeck. 1998. Visualization of quasi-2D unsaturated flow during dynamic outflow experiments. *Am. Geophys. Union. Eos Trans.* 79:368.
- Mualem, Y. 1976. A new model for predicting the hydraulic conductivity of unsaturated porous media. *Water Resour. Res.* 12:513–522.
- Nielsen, D.R., J.W. Biggar, and J.M. Davidson. 1962. Experimental consideration of diffusion analysis in unsaturated flow problems. *Soil Sci. Soc. Am. Proc.* 26:107–111.

- Nielsen, D.R., M.Th. van Genuchten, and J.W. Biggar. 1986. Water flow and solute transport processes in the unsaturated zone. *Water Resour. Res.* 22:89S–108S.
- Parker, J.C., J.B. Kool, and M.Th. van Genuchten. 1985. Determining soil hydraulic properties from one-step outflow experiments by parameter estimation. II. Experimental studies. *Soil Sci. Soc. Am. J.* 49:1354–1359.
- Passioura, J.B. 1976. Determining soil water diffusivities from one-step outflow experiments. *Austr. J. Soil Res.* 15:1–8.
- Perroux, K.M., and I. White. 1968. Design for disc permeameters. *Soil Sci. Soc. Am. J.* 52:1205–1215.
- Quintard, M., and S. Whitaker. 1999. Fundamentals of transport equation formulation for two-phase flow in homogeneous and heterogeneous porous media. p. 3–57. *In* M.B. Parlange and J.W. Hopmans (ed.) *Vadose zone hydrology: Cutting across disciplines*. Oxford University Press, Oxford, UK.
- Reynolds, W.D., and D.E. Elrick. 1991. Determination of hydraulic conductivity using a tension infiltrometer. *Soil Sci. Soc. Am. J.* 55:633–639.
- Reynolds, W.D., and W.D. Zebhek. 1996. Use of contact material in tension infiltrometer measurements. *Soil Technol.* 9:141–159.
- Reeve, M.J., and A.D. Carter. 1991. Water release characteristic. p. 111–160. *In* K.A. Smith and C.E. Mullins (ed.) *Soil analysis: Physical methods*. Marcel Dekker, New York, NY.
- Romano, N. 1993. Use of an inverse method and geostatistics to estimate soil hydraulic conductivity for spatial variability analysis. *Geoderma* 60:169–186.
- Romano, N., and A. Santini. 1999. Determining soil hydraulic functions from evaporation experiments by a parameter estimation approach: Experimental verifications and numerical studies. *Water Resour. Res.* 35:3343–3359.
- Russo, D. 1988. Determining soil hydraulic properties by parameter estimation: On the selection of a model for the hydraulic properties. *Water Resour. Res.* 24:453–459.
- Russo, D., E. Bresler, U. Shani, and J.C. Parker. 1991. Analysis of infiltration events in relation to determining soil hydraulic properties by inverse problem methodology. *Water Resour. Res.* 27:1361–1373.
- Santini, A., and N. Romano. 1992. A field method for determining soil hydraulic properties. Proceedings of XXIII Congress of Hydraulics and Hydraulic Constructions. Florence, Italy. 31 Aug.–4 Sept. Tecnoprint S.n.c., Bologna, I:B.117–B.139 (in Italian; available also in English).
- Santini, A., N. Romano, G. Ciollaro, and V. Comegna. 1995. Evaluation of a laboratory inverse method for determining unsaturated hydraulic properties of a soil under different tillage practices. *Soil Sci.* 160:340–351.
- Schaap, M.G., and F.J. Leij. 2000. Improved prediction of unsaturated hydraulic conductivity with the Mualem–van Genuchten model. *Soil Sci. Soc. Am. J.* 64:843–851.
- Schindler, U. 1980. Ein Schnellverfahren zur Messung der Wasserleitfähigkeit im teilgesättigten Boden an Stechzylinderproben. *Arch. Acker-Pflanzenbau u. Bodenkd.* 24:1–7.
- Schultze, B., O. Ippisch, B. Huwe, and W. Durner. 1999. Dynamic nonequilibrium in unsaturated water flow. p. 877–892. *In* M.Th. van Genuchten et al. (ed.) *Characterization and measurement of the hydraulic properties of unsaturated porous media*. University of California, Riverside, CA.
- Schultze, B., T. Zurmühl, and W. Durner. 1996. Untersuchung der Hysterese hydraulischer Funktionen von Böden mittels inverser Simulation. *Mitteilungen der Deutschen Bodenkundlichen Gesellschaft* 80:319–322.
- Šimůnek, J., R. Angulo-Jaramillo, M.G. Schaap, J.-P. Vandervaere, and M.Th. van Genuchten. 1998a. Using an inverse method to estimate the hydraulic properties of crusted soils from tension disc infiltrometer data. *Geoderma* 86:61–81.
- Šimůnek, J., J.W. Hopmans, D.R. Nielsen, and M.Th. van Genuchten. 2000. Horizontal infiltration revisited using parameter optimization. *Soil Sci.* 165:708–717.
- Šimůnek, J., R. Kodešová, M.M. Gribb, and M.Th. van Genuchten. 1999a. Estimating hysteresis in the soil water retention function from modified cone penetrometer test. *Water Resour. Res.* 35:1329–1345.
- Šimůnek, J., M. Šejna, and M.Th. van Genuchten. 1998b. The HYDRUS-1D software package for simulating the one-dimensional movement of water, heat, and multiple solutes in variably-saturated media. Version 2.0. IGWMC-TPS-70. International Ground Water Modeling Center, Colorado School of Mines, Golden, CO.
- Šimůnek, J., M. Šejna, and M.Th. van Genuchten. 1999b. The HYDRUS-2D software package for simulating two-dimensional movement of water, heat, and multiple solutes in variably-saturated media. Version 2.0. IGWMC-TPS-53. International Ground Water Modeling Center, Colorado School of Mines, Golden, CO.
- Šimůnek, J., and M.Th. van Genuchten. 1996. Estimating unsaturated soil hydraulic properties from tension disc infiltrometer data by numerical inversion. *Water Resour. Res.* 32:2683–2696.

- Šimůnek, J., and M.Th. van Genuchten. 1997. Estimating unsaturated soil hydraulic properties from multiple tension disc infiltrometer data. *Soil Sci.* 162:383–398.
- Šimůnek, J., and M.Th. van Genuchten. 2000. The DISC computer software for analyzing tension disc infiltrometer data by parameter estimation. Versions 1.0. Research Rep. 145. U.S. Salinity Laboratory, USDA-ARS, Riverside, CA.
- Šimůnek, J., O. Wendroth, and M.Th. van Genuchten. 1998c. A parameter estimation analysis of the evaporation method for determining soil hydraulic properties. *Soil Sci. Soc. Am. J.* 62:894–905.
- Šimůnek, J., O. Wendroth, and M.Th. van Genuchten. 1999c. Estimating soil hydraulic properties from laboratory evaporation experiments by parameter estimation. p. 713–724. *In* M.Th. van Genuchten et al. (ed.) *Characterization and measurement of the hydraulic properties of unsaturated porous media*. University of California, Riverside, CA.
- Šimůnek, J., O. Wendroth, and M.Th. van Genuchten. 1999d. A parameter estimation analysis of the laboratory tension disc experiment for determining soil hydraulic properties. *Water Resour. Res.* 35:2965–2979.
- Šimůnek, J., O. Wendroth, N. Wypler, and M.Th. van Genuchten. 2001. Nonequilibrium water flow characterized from an upward infiltration experiment. *Eur. J. Soil Sci.* 52:13–24.
- Smettem, K.R.J., and B.E. Clothier. 1989. Measuring unsaturated sorptivity and hydraulic conductivity using multiple disk permeameters. *J. Soil Sci.* 40:563–568.
- Tamari, S., L. Bruckler, J. Halbertsma, and J. Chadoeuf. 1993. A simple method for determining soil hydraulic properties in the laboratory. *Soil Sci. Soc. Am. J.* 57:642–651.
- Toorman, A.F., P.J. Wierenga, and R.G. Hills. 1992. Parameter estimation of soil hydraulic properties from one-step outflow data. *Water Resour. Res.* 28:3021–3028.
- Topp, G.C., and J.L. Davis. 1985. Measurement of soil water content using time domain reflectometry (TDR). *Soil Sci. Soc. Am. J.* 46:19–24.
- Vachaud, G., C. Dancette, S. Sonko, and J.L. Thony. 1978. Méthodes de caractérisation hydrodynamique in situ d'un sol non saturé. Application à deux types de sol du Sénégal en vue de la détermination des termes du bilan hydrique. *Ann. Agron.* 29:1–36.
- Valiantzas, J.D., and D.G. Kerkides. 1990. A simple iterative method for the simultaneous determination of soil hydraulic properties from one-step outflow data. *Water Resour. Res.* 26:143–152.
- van Dam, J.C., J.N.M. Stricker, and P. Droogers. 1992. Evaluation of the inverse method for determining soil hydraulic functions from one-step outflow experiments. *Soil Sci. Soc. Am. J.* 56:1042–1050.
- van Dam, J.C., J.N.M. Stricker, and P. Droogers. 1994. Inverse method for determining soil hydraulic functions from multi-step outflow experiments. *Soil Sci. Soc. Am. J.* 58:647–652.
- van Genuchten, M.Th. 1980. A closed-form equation for predicting the hydraulic conductivity of unsaturated soils. *Soil Sci. Soc. Am. J.* 44:892–898.
- van Genuchten, M.Th., and E.A. Sudicky. 1999. Recent advances in vadose zone flow and transport modeling. p. 155–193. *In* M.B. Parlange and J.W. Hopmans (ed.) *Vadose zone hydrology: Cutting across disciplines*. Oxford University Press, Oxford, UK.
- Vogel, T., M. Nahaei, and M. Císlarová. 1999. Description of soil hydraulic properties near saturation from the point of view of inverse modeling. p. 693–703. *In* M.Th. van Genuchten et al. (ed.) *Characterization and measurement of the hydraulic properties of unsaturated porous media*. University of California, Riverside, CA.
- Vrugt, J., J.W. Hopmans, and J. Šimůnek. 2001a. Calibration of a two-dimensional root water uptake model. *Soil Sci. Soc. Am. J.* 65:1027–1037.
- Vrugt, J., A. Weerts, and W. Bouten. 2001b. Information content of data for identifying soil hydraulic properties from outflow experiments. *Soil Sci. Soc. Am. J.* 65:19–27.
- Wang, D., S.R. Yates, and F. F. Ernst. 1998. Determining soil hydraulic properties using tension infiltrometers, time domain reflectometry, and tensiometers. *Soil Sci. Soc. Am. J.* 62:318–325.
- Wendroth, O., W. Ehlers, J.W. Hopmans, H. Kage, J. Halbertsma, and J.H.M. Wösten. 1993. Reevaluation of the evaporation method for determining hydraulic functions in unsaturated soils. *Soil Sci. Soc. Am. J.* 57:1436–1443.
- Whisler, F.D., and K.K. Watson. 1968. One-dimensional gravity drainage of uniform columns of porous materials. *J. Hydrol.* 6:277–296.
- White, I., and M.J. Sully. 1987. Macroscopic and microscopic capillary length and time scales from field infiltration. *Water Resour. Res.* 23:1514–1522.
- Wildenschild, D., J.W. Hopmans, and J. Šimůnek. 2001. Flow rate dependence of soil hydraulic characteristics. *Soil Sci. Soc. Am. J.* 65:35–48.
- Wildenschild, D., K.H. Jensen, K.J. Hollenbeck, T.H. Illangasekare, D. Znidarcic, T. Sonnenborg, and M.B. Butts. 1997. A two-stage procedure for determining unsaturated hydraulic characteristics using a syringe pump and outflow observations. *Soil Sci. Soc. Am. J.* 61:347–359.

- Wind, G. P. 1968. Capillary conductivity data estimated by a simple method. p. 181–191. *In* P.E. Rijtema and H. Wassink (ed.) *Water in the unsaturated zone*. Proc. Wageningen Symp. June 1966. Vol. 1. IASAH, Gentbrugge, Belgium.
- Wooding, R.A. 1968. Steady infiltration from large shallow circular pond. *Water Resour. Res.* 4:1259–1273.
- Zachmann, D.W., P.C. Duchateau, and A. Klute. 1981. The calibration of Richards flow equation for a draining column by parameter identification. *Soil Sci. Soc. Am. J.* 45:1012–1015.
- Zachmann, D.W., P.C. Duchateau, and A. Klute. 1982. Simultaneous approximation of water capacity and soil hydraulic conductivity by parameter identification. *Soil Sci.* 134:157–163.
- Zijlstra, J., and J.H. Dane. 1996. Identification of hydraulic parameters in layered soils based on a quasi-Newton method. *J. Hydrol.* 181:233–250.
- Zurmühl, T. 1998. Capability of convection dispersion transport models to predict transient water and solute movement in undisturbed soil columns. *J. Contam. Hydrol.* 30:99–126.
- Zurmühl, T., and W. Durner. 1998. Determination of parameters for bimodal hydraulic functions by inverse modeling. *Soil Sci. Soc. Am. J.* 62:874–880.